

# Stochastic foundations of undulatory transport phenomena: Generalized Poisson-Kac processes - Part II Irreversibility, Norms and Entropies

Massimiliano Giona<sup>\*1</sup>, Antonio Brasiello<sup>2</sup>, and Silvestro Crescitelli<sup>3</sup>

<sup>1</sup>Dipartimento di Ingegneria Chimica DICMA Facoltà di Ingegneria,  
La Sapienza Università di Roma via Eudossiana 18, 00184, Roma,  
Italy

\* Email: massimiliano.giona@uniroma1.it

<sup>2</sup>Dipartimento di Ingegneria Industriale Università degli Studi di  
Salerno via Giovanni Paolo II 132, 84084 Fisciano (SA), Italy

<sup>3</sup>Dipartimento di Ingegneria Chimica, dei Materiali e della  
Produzione Industriale Università degli Studi di Napoli “Federico II”  
piazzale Tecchio 80, 80125 Napoli, Italy

## Abstract

In this second part, we analyze the dissipation properties of Generalized Poisson-Kac (GPK) processes, considering the decay of suitable  $L^2$ -norms and the definition of entropy functions. In both cases, consistent energy dissipation and entropy functions depend on the whole system of primitive statistical variables, the partial probability density functions  $\{p_\alpha(\mathbf{x}, t)\}_{\alpha=1}^N$ , while the corresponding energy dissipation and entropy functions based on the overall probability density  $p(\mathbf{x}, t)$  do not satisfy monotonicity requirements as a function of time. Examples from chaotic advection (standard map coupled to stochastic GPK processes) illustrate this phenomenon. Some complementary physical issues are also addressed: the ergodicity breaking in the presence of attractive potentials, and the use of GPK perturbations to mollify stochastic field equations.

## 1 Introduction

The setting of Generalized Poisson-Kac processes (GPK, for short) has been addressed in detail in part I [1], explaining their physical motivation, as a generalization of the Kac’s paradigm of stochastic processes possessing finite propagation velocity [2], and their structural properties with particular emphasis on the Kac limit. In point of fact, the Kac limit represents a form of

asymptotic consistency of GPK stochastic differential equations with respect to classical Langevin equation driven by Wiener processes (which can be also referred to as the *Brownian motion consistency of GPK processes*). We refer to part I for the notation and the basic properties of GPK dynamics that are not reviewed here to avoid repetition.

In this second part of the work we focus on the characterization of irreversibility in GPK dynamics, essentially grounded on the definition of suitable  $L^2$ -norms (energy dissipation functions) based on the system of the partial probability density functions  $p_\alpha(\mathbf{x}, t)$ ,  $\alpha = 1, \dots, N$ , and possessing a monotonic decay in time, and of proper entropy functions for GPK processes. Section 2 is entirely dedicated to this issue. In both cases, dissipation and entropy functions can be defined for GPK processes of increasing structural complexity and depend on the whole system of partial probability waves. Starting from the simplest cases, we consider transitionally symmetric GPK processes [1] and extend the analysis to the transitionally non-symmetric case, admitting relativistic implications.

Moreover, energy dissipation and entropy functions constructed solely upon the knowledge of the overall probability density  $p(\mathbf{x}, t) = \sum_{\alpha=1}^N p_\alpha(\mathbf{x}, t)$  do not satisfy the requirement of monotonicity in time, and consequently are thermodynamically inconsistent. This is a first important physical indication on the fact that the primitive statistical description of GPK processes is entirely based on the whole set of partial probability waves and cannot be reduced to the coarser description based on the overall probability density function  $p(\mathbf{x}, t)$  and its associated probability density flux  $\mathbf{J}_d(\mathbf{x}, t)$ , see part I. This result is fully consistent with the underlying hypothesis of extended thermodynamic theories [3, 4, 5], and indicates that GPK processes are the simplest candidate for the microdynamic equations of motion in extended theory of far-from-equilibrium phenomena. This issue is further elaborated in part III [6].

A physically meaningful example illustrating these properties refers to chaotic advection of tracer particles in the presence of a stochastic perturbation (diffusion), modelled as a GPK process. As a prototypical model flow we consider the continuous-time flow associated with the standard map [7, 8] on the two-dimensional torus (Section 3).

Finally Section 4 addresses some auxiliary physical properties of GPK processes: (i) the use of GPK perturbations to mollify stochastic field equations (stochastic partial differential equations) [9, 10], and (ii) the occurrence of ergodicity breaking in the presence of attractive potentials. The analysis of one-dimensional models addressed in [11] is briefly reviewed, and the theory is extended to higher-dimensional systems.

## 2 Norm dynamics, fluxes and entropy

The definition and evolution of suitable  $L^2$ -norms accounting for the dissipation induced by stochasticity is strictly connected with the setting of a proper entropy function. Both the definition of an energy-dissipation function, based on the  $L^2$ -norms of the characteristic partial probability waves, and that of an entropy function depend not solely on the overall probability density function  $p(\mathbf{x}, t)$ , as for Wiener-driven Langevin equations, but also on other dynamic quantities describing the process. These quantities are simply the diffusive flux in the one-dimensional Poisson-Kac process, or a combination of fluxes and other auxiliary quantities in the general GPK case. The analysis of the GPK case reveals that the use of primitive statistical quantities, i.e., of the partial probability waves, provides the simplest and physically meaningful description of dissipation.

The exposition is organized as follows. To begin with, the one-dimensional Poisson-Kac process in the absence of deterministic biasing fields is addressed. Subsequently, the case of GPK processes is thoroughly treated, starting from simpler cases up to the more general case of transitionally non-symmetric GPK dynamics. The latter case is relevant in connection with the relativistic setting of GPK dynamics, and with their transformation properties under a Lorentz boost.

### 2.1 One-dimensional Poisson-Kac diffusion

Consider the one-dimensional Poisson-Kac process in the absence of a deterministic bias, i.e.,  $dx(t) = b(-1)^{\chi(t)}$ , where the Poisson process  $\chi(t)$  is characterized by the transition rate  $\lambda > 0$ . In the Kac limit, it corresponds to a purely diffusive Brownian motion, possessing an effective diffusivity  $D_{\text{eff}} = b^2/2\lambda$ . Its statistical description involves the two partial probability waves  $p^\pm(x, t)$ , satisfying the hyperbolic system of equation

$$\partial_t p^\pm(x, t) = \mp b \partial_x p^\pm(x, t) \mp \lambda [p^+(x, t) - p^-(x, t)] \quad (1)$$

An energy-dissipation function of the process  $\mathcal{E}_d[p^+, p^-](t)$  is a bilinear functional of the partial probability densities  $p^+(x, t)$ ,  $p^-(x, t)$ ,

$$\mathcal{E}_d(t) = \mathcal{E}_d[p^+, p^-](t) = \sum_{\alpha, \beta = \pm} C_{\alpha, \beta} \int p^\alpha(x, t) p^\beta(x, t) dx \quad (2)$$

where  $C_{\alpha, \beta}$  are non-negative constants, such that along the evolution of the process

$$\frac{d\mathcal{E}_d(t)}{dt} \leq 0 \quad (3)$$

where, for notational simplicity, the explicit dependence on the partial waves has been omitted.

Consider the unbounded propagation in  $x \in (-\infty, \infty)$ . In order to obtain an expression for  $\mathcal{E}_d(t)$  take the system of eqs. (1), multiply the evolution equation for  $p^+(x, t)$  by  $p^+(x, t)$ , and that for  $p^-(x, t)$  by  $p^-(x, t)$ , sum them together, and integrate over  $x$ ,

$$\begin{aligned} \frac{1}{2} \frac{d}{dt} \int_{-\infty}^{\infty} [(p^+)^2 + (p^-)^2] dx &= -\frac{b}{2} \int_{-\infty}^{\infty} \partial_x [(p^+)^2 - (p^-)^2] dx \\ &\quad - \lambda \int_{-\infty}^{\infty} (p^+ - p^-)^2 dx \end{aligned} \quad (4)$$

where the regularity conditions at infinity have been enforced. This means that an energy-dissipation function can be defined as

$$\mathcal{E}_d(t) = \frac{1}{2} \int_{-\infty}^{\infty} [(p^+)^2 + (p^-)^2] dx \quad (5)$$

and eq. (4) implies that

$$\frac{d\mathcal{E}_d(t)}{dt} = -\frac{\lambda}{b^2} \|J_d\|_{L^2}^2(t) \quad (6)$$

where  $\|f\|_{L^2}^2(t)$ , for a real-valued square summable function  $f(x, t)$ , is the square of its  $L^2$ -norm  $\|f\|_{L^2}^2(t) = \int_{-\infty}^{\infty} f^2(x, t) dx$ . Since  $p^\pm = (p \pm J_d)/2$ ,  $\mathcal{E}_d(t)$  can be expressed as

$$\mathcal{E}_d = \frac{1}{4} \int_{-\infty}^{\infty} \left( p^2 + \frac{J_d^2}{b^2} \right) dx \quad (7)$$

i.e., it is a quadratic functional of both the overall probability density function  $p(x, t)$  and of its diffusive flux  $J_d(x, t)$ . In the Kac limit,  $\lambda/b^2 = 1/2D_{\text{eff}}$ ,  $J_d(x, t) = -D_{\text{eff}} \partial_x p(x, t)$ , and eq. (6) reduces to the classical Fickian dissipation relation  $\partial_t \|p\|_{L^2}^2 = -2D_{\text{eff}} \|\partial_x p\|_{L^2}^2$ . The remarkable property of eq. (6) is that the energy dissipation function depends also on the flux, which is the fundamental starting point in the theory of extended irreversible thermodynamics.

Next consider, instead of unbounded propagation, a closed interval  $x \in [0, L]$ , where zero-flux conditions applies at the boundaries  $x = 0, L$ . These conditions correspond to the reflection conditions  $p^+|_{x=0} = p^-|_{x=0}$ ,  $p^-|_{x=L} = p^+|_{x=L}$  for the partial probability waves. Eq. (4) holds also in this case, substituting the integration extremes  $x = -\infty$  and  $x = \infty$  with  $x = 0$  and  $x = L$ , respectively. Observe that the reflection conditions make the divergence integral appearing in eq. (4) identically equal to zero, so that eqs. (6)-(7) hold true also in this case, substituting the integration extremes  $-\infty$  and  $\infty$  with 0 and  $L$ , respectively.

Next, consider the entropy function. As a candidate for entropy consider the Boltzmann-Shannon entropy  $S_{BS}(t)$  defined with respect to the partial

probability waves. In the case of unbounded propagation it reads

$$S_{BS}(t) = - \int_{-\infty}^{\infty} [p^+ \log p^+ + p^- \log p^-] dx \quad (8)$$

Enforcing the balance equations for the partial waves, one obtains

$$\begin{aligned} \frac{dS_{BS}(t)}{dt} &= -b \int_{-\infty}^{\infty} \partial_x [p^+ \log p^+ - p^- \log p^- - p^+ + p^-] dx \\ &= \lambda \int_{-\infty}^{\infty} (p^+ - p^-) \log \left( \frac{p^+}{p^-} \right) dx \end{aligned} \quad (9)$$

The divergence integral vanishes because of the regularity conditions at infinity, so that

$$\frac{dS_{BS}(t)}{dt} = \lambda \int_{-\infty}^{\infty} (p^+ - p^-) \log \left( \frac{p^+}{p^-} \right) dx \geq 0 \quad (10)$$

since the function  $g(x, y) = (x - y) \log(x/y)$  is non negative for  $x, y \geq 0$ . An analogous result holds in a closed bounded system represented by the interval  $[0, L]$ , in the presence of reflecting boundary conditions for the partial waves, substituting the integral from  $-\infty$  to  $\infty$  with an integral from 0 to  $L$

The first analytical results for the entropy function in the presence of a hyperbolic Cattaneo transport model have been derived by Camacho and Jou [12], exhibiting a quadratic dependence on the probability flux, and reducing under equilibrium condition to the Boltzmann  $H$ -function. This result has been generalized by Vlad and Ross for telegrapher-type master equations [13]. A recent survey on the entropy principle related with extended thermodynamic formulations can be found in [14].

## 2.2 GPK processes

The analysis of dissipation functions and entropies in GPK processes is essentially related to the underlying Markov-chain structure of the finite  $N$ -state Poisson process generating stochasticity in the system. The key role is played by the spectral properties of the transition matrix  $\mathbf{A}$  which, in the general setting, is simply an irreducible left-stochastic matrix  $A_{\alpha,\beta} \geq 0$ ,  $\sum_{\gamma=1}^N A_{\gamma,\alpha} = 1$ ,  $\alpha = 1, \dots, N$ . The spectral properties of  $\mathbf{A}$  that are relevant in the remainder are: (i) the spectral radius of  $\mathbf{A}$  is 1 [15], i.e., all the eigenvalues  $\mu_\alpha$ ,  $\alpha = 1, \dots, N$  of  $\mathbf{A}$ , i.e.,  $\sum_{\beta=1}^N A_{\alpha,\beta} c_\beta = \mu_\alpha c_\alpha$ , are such that  $|\mu_\alpha| \leq 1$ ; (ii) the dominant Frobenius eigenvalue is  $\mu = 1$ , corresponding to a uniform left eigenvector (all the entries are equal); (iii) for  $\alpha = 2, \dots, N$ ,  $\mu_\alpha < 1$ .

From part I we know that the statistical description of a GPK process defined by  $N$  distinct constant stochastic velocity vectors  $\mathbf{b}_\alpha$ ,  $\alpha = 1, \dots, N$ , in the presence of a deterministic velocity field  $\mathbf{v}(\mathbf{x})$ , involves  $N$  partial

probability density functions  $p_\alpha(\mathbf{x}, t)$ ,  $\alpha = 1, \dots, N$  satisfying the hyperbolic system of equations

$$\partial_t p_\alpha(\mathbf{x}, t) = -\nabla \cdot [(\mathbf{v}(\mathbf{x}) + \mathbf{b}_\alpha) p_\alpha(\mathbf{x}, t)] - \lambda_\alpha p_\alpha(\mathbf{x}, t) + \sum_{\gamma=1}^N \lambda_\gamma A_{\alpha,\gamma} p_\gamma(\mathbf{x}, t) \quad (11)$$

Throughout this paragraph, we assume for simplicity that the deterministic velocity field  $\mathbf{v}(\mathbf{x})$  is solenoidal, i.e.,  $\nabla \cdot \mathbf{v}(\mathbf{x}) = 0$ . This condition, with some further technical efforts, could be removed, at least for some classes of potential and mixed flows. The generalization to generic irrotational velocity fields (potential flows) is left open, and is not as simple as it may seem, for technical reasons that are briefly addressed in Section 4.

The analysis of energy dissipation and entropy functions for GPK processes is developed gradually by considering classes of processes of increasing structural complexity, defined by the symmetry properties of  $\mathcal{B}_N$ ,  $\mathbf{A}$  and  $\mathbf{\Lambda}$  (see part I).

To begin with, consider the simplest case of a transitionally symmetric GPK process possessing a uniform transition rate vector  $\mathbf{\Lambda} = (\lambda, \dots, \lambda)$ . In this, case the transition probability matrix  $\mathbf{A}$  is also symmetric. For this class of processes, an energy dissipation function is given by

$$\mathcal{E}_d[\{p_\alpha\}_{\alpha=1}^N](t) = \frac{1}{2} \sum_{\alpha=1}^N \int_{\mathbb{R}^n} p_\alpha^2(\mathbf{x}, t) d\mathbf{x} \quad (12)$$

To prove this, multiply each balance equation for the corresponding partial wave  $p_\alpha(\mathbf{x}, t)$ , sum over the states  $\alpha$  and integrated with respect to  $\mathbf{x}$  to obtain

$$\begin{aligned} \frac{d\mathcal{E}_d(t)}{dt} &= - \sum_{\alpha=1}^N \int_{\mathbb{R}^n} p_\alpha \nabla \cdot (\mathbf{v} p_\alpha) d\mathbf{x} - \sum_{\alpha=1}^N \int_{\mathbb{R}^n} p_\alpha \nabla \cdot (\mathbf{b}_\alpha p_\alpha) d\mathbf{x} \\ &\quad - \lambda \sum_{\alpha=1}^N \int_{\mathbb{R}^n} p_\alpha^2 d\mathbf{x} + \lambda \sum_{\alpha,\gamma=1}^N \int_{\mathbb{R}^n} p_\alpha A_{\alpha,\gamma} p_\gamma d\mathbf{x} \end{aligned} \quad (13)$$

The first two integrals vanish as they can be expressed in a divergence form,  $p_\alpha \nabla \cdot (\mathbf{v} p_\alpha) = \nabla \cdot (\mathbf{v} p_\alpha^2/2)$ ,  $p_\alpha \nabla \cdot (\mathbf{b}_\alpha p_\alpha) = \nabla \cdot (\mathbf{b}_\alpha p_\alpha^2/2)$ , and regularity conditions at infinity apply.

Indicating with  $(\mathbf{f}, \mathbf{g})_{L_N^2}$  the scalar product for  $N$ -dimensional real-valued square summable functions  $\mathbf{f}(\mathbf{x}) = (f_1(\mathbf{x}), \dots, f_N(\mathbf{x}))$ ,  $\mathbf{g}(\mathbf{x}) = (g_1(\mathbf{x}), \dots, g_N(\mathbf{x}))$  of  $\mathbb{R}^n$ ,

$$(\mathbf{f}, \mathbf{g})_{L_N^2} = \sum_{\alpha=1}^N \int_{\mathbb{R}^n} f_\alpha(\mathbf{x}) g_\alpha(\mathbf{x}) d\mathbf{x} \quad (14)$$

eq. (13) can be expressed as

$$\frac{1}{\lambda} \frac{d\mathcal{E}_d(t)}{dt} = -(\mathbf{p}, \mathbf{p})_{L_N^2} + (\mathbf{A} \mathbf{p}, \mathbf{p})_{L_N^2} \quad (15)$$

where  $\mathbf{p}(\mathbf{x}, t) = (p_1(\mathbf{x}, t), \dots, p_N(\mathbf{x}, t))$  is the vector of the partial probability waves. Since the maximum (Frobenius) eigenvalue of  $\mathbf{A}$  equals 1, and all the other eigenvalues lie within the unit circle and possess real parts less than 1, it follows that

$$|(\mathbf{A} \mathbf{p}, \mathbf{p})_{L_N^2}| \leq (\mathbf{p}, \mathbf{p})_{L_N^2} \quad (16)$$

and consequently, eq. (15) provides the inequality

$$\frac{d\mathcal{E}_d(t)}{dt} \leq 0 \quad (17)$$

As regards the entropy function, one can consider the Boltzmann-Shannon expression defined starting from the partial probability waves characterizing the process

$$S_{BS}(t) = - \sum_{\alpha=1}^N \int_{\mathbb{R}^n} p_{\alpha}(\mathbf{x}, t) \log p_{\alpha}(\mathbf{x}, t) d\mathbf{x} \quad (18)$$

Enforcing the conservation property  $\sum_{\alpha=1}^N \int_{\mathbb{R}^n} p_{\alpha}(\mathbf{x}, t) d\mathbf{x} = 1$ , and simplifying the resulting expression as regards the divergence terms that are vanishing because of the regularity at infinity, one finally obtains

$$\begin{aligned} \frac{dS_{BS}(t)}{dt} &= \lambda \left[ \sum_{\alpha=1}^N \int_{\mathbb{R}^n} p_{\alpha} \log p_{\alpha} d\mathbf{x} - \sum_{\alpha, \gamma=1}^N \int_{\mathbb{R}^n} \log p_{\alpha} A_{\alpha, \gamma} p_{\gamma} d\mathbf{x} \right] \\ &= \lambda \left[ (\mathbf{p}, \log \mathbf{p})_{L_N^2} - (\mathbf{A} \mathbf{p}, \log \mathbf{p})_{L_N^2} \right] \end{aligned} \quad (19)$$

where we have set  $\log \mathbf{p} = (\log p_1, \dots, \log p_N)$ . The term at the right-hand side of eq. (19) equals  $\lambda$  times the integral over  $\mathbf{x}$  of a function  $g_S(\mathbf{p})$ , i.e.,  $dS_{BS}(t)/dt = \lambda \int_{\mathbb{R}^n} g_S(\mathbf{p}(\mathbf{x}, t)) d\mathbf{x}$ , given by

$$\begin{aligned} g_S(\mathbf{p}) &= \frac{1}{2} \sum_{\alpha, \gamma=1}^N A_{\alpha, \gamma} (p_{\alpha} - p_{\gamma}) \log \left( \frac{p_{\alpha}}{p_{\gamma}} \right) \\ &= \frac{1}{2} \left[ \sum_{\alpha, \gamma=1}^N A_{\alpha, \gamma} p_{\alpha} \log p_{\alpha} - \sum_{\alpha, \gamma=1}^N A_{\alpha, \gamma} p_{\gamma} \log p_{\alpha} \right. \\ &\quad \left. - \sum_{\alpha, \gamma=1}^N A_{\alpha, \gamma} p_{\alpha} \log p_{\gamma} + \sum_{\alpha, \gamma=1}^N A_{\alpha, \gamma} p_{\gamma} \log p_{\gamma} \right] \\ &= \sum_{\alpha=1}^N p_{\alpha} \log p_{\alpha} - \sum_{\alpha, \gamma=1}^N \log p_{\alpha} A_{\alpha, \gamma} p_{\gamma} \end{aligned} \quad (20)$$

where the symmetry of  $A_{\alpha,\gamma}$  and its left stochasticity have been enforced. Since  $A_{\alpha,\gamma} \geq 0$ , and each factor  $(p_\alpha - p_\gamma) \log(p_\alpha/p_\gamma)$  is greater than or at most equal to zero for  $p_\alpha(\mathbf{x}, t), p_\gamma(\mathbf{x}, t) \geq 0$ , it follows that

$$\frac{dS_{BS}(t)}{dt} \geq 0 \quad (21)$$

Next, consider the general case in the presence of an arbitrary distribution of transition rate  $\lambda_\alpha$ ,  $\alpha = 1, \dots, N$ . As regards the energy-dissipation function, it is convenient to introduce the auxiliary functions  $u_\alpha(\mathbf{x}, t)$  defined as

$$u_\alpha(\mathbf{x}, t) = \lambda_\alpha p_\alpha(\mathbf{x}, t), \quad \alpha = 1, \dots, N \quad (22)$$

In terms of the  $u_\alpha$ 's, the balance equations (11) become

$$\lambda_\alpha^{-1} \partial_t u_\alpha = -\lambda_\alpha^{-1} \nabla \cdot (\mathbf{v} u_\alpha) - \lambda_\alpha^{-1} \nabla \cdot (\mathbf{b}_\alpha u_\alpha) - u_\alpha + \sum_{\gamma=1}^N A_{\alpha,\gamma} u_\gamma \quad (23)$$

$\alpha = 1, \dots, N$ . It is natural to introduce the following energy dissipation function

$$\mathcal{E}_d[\{p_\alpha\}_{\alpha=1}^N](t) = \sum_{\alpha=1}^N \frac{1}{2\lambda_\alpha} \int_{\mathbb{R}^n} u_\alpha^2(\mathbf{x}, t) d\mathbf{x} = \sum_{\alpha=1}^N \frac{\lambda_\alpha}{2} \int_{\mathbb{R}^n} p_\alpha^2(\mathbf{x}, t) d\mathbf{x} \quad (24)$$

Performing the same algebra as in the previous case and setting  $\mathbf{u} = (u_1, \dots, u_N)$ , one obtains

$$\frac{d\mathcal{E}_d(t)}{dt} = -(\mathbf{u}, \mathbf{u})_{L_N^2} + (\mathbf{A} \mathbf{u}, \mathbf{u})_{L_N^2} \leq 0 \quad (25)$$

that follows from the fact that  $\mathbf{A}$  is left-stochastic. Observe that no assumptions has been made on the symmetry of the transition matrix  $K_{\alpha,\gamma} = \lambda_\gamma A_{\alpha,\gamma}$  so that eqs. (24) apply both for transitionally symmetric and non-symmetric GPK processes.

Next, consider the entropy. As regards the entropy function, the local detailed balance defining transitionally symmetric GPK processes counts. To begin with, consider transitionally symmetric GPK processes, characterized by the property that the transition matrix  $\mathbf{K} = \mathbf{A} \mathbf{\Lambda}$  is symmetric, i.e.,

$$K_{\alpha,\gamma} = \lambda_\gamma A_{\alpha,\gamma} = \lambda_\alpha A_{\gamma,\alpha} = K_{\gamma,\alpha}, \quad \alpha, \gamma = 1, \dots, N \quad (26)$$

with the property that  $K_{\alpha,\gamma} \geq 0$  and

$$\sum_{\gamma=1}^N K_{\gamma,\alpha} = \lambda_\alpha \quad (27)$$

For transitionally symmetric GPK processes the expression (18) for the Boltzmann-Shannon entropy is still a valid candidate as the entropy function



of the process. Enforcing the properties (26)-(27) of the transition matrix  $\mathbf{K}$ , the time derivative of the Boltzmann-Shannon entropy becomes

$$\frac{dS_{BS}(t)}{dt} = \int_{\mathbb{R}^n} \sum_{\alpha, \gamma=1}^N K_{\alpha, \gamma} [p_{\alpha}(\mathbf{x}, t) - p_{\gamma}(\mathbf{x}, t)] \log p_{\alpha}(\mathbf{x}, t) d\mathbf{x} \quad (28)$$

The latter expression can be written in terms of a entropy-rate density  $r_S(\mathbf{p}(\mathbf{x}, t))$ , i.e., as  $dS_{BS}(t)/dt = \int_{\mathbb{R}^n} r_S(\mathbf{p}(\mathbf{x}, t)) d\mathbf{x}$ , given by

$$r_S(\mathbf{p}) = \frac{1}{2} \sum_{\alpha, \gamma=1}^N K_{\alpha, \gamma} (p_{\alpha} - p_{\gamma}) \log \left( \frac{p_{\alpha}}{p_{\gamma}} \right) \quad (29)$$

which, by definition, is greater than or at most equal to zero for any  $p_{\alpha}(\mathbf{x}, t) \geq 0$ ,  $\alpha = 1, \dots, N$ .

There is another situation of physical interest (see further paragraph 2.4), namely when the transition probability matrix  $A_{\alpha, \gamma}$  is symmetric, but the transition rates  $\lambda_{\alpha}$ ,  $\alpha = 1, \dots, N$  are arbitrary positive constants. The resulting GPK process is therefore transitionally non-symmetric. In this case, one can define a modified Boltzmann-Shannon entropy  $\hat{S}_{BS}(t)$  as

$$\hat{S}_{BS}(t) = - \sum_{\alpha=1}^N \frac{1}{\lambda_{\alpha}} \int_{\mathbb{R}^n} u_{\alpha}(\mathbf{x}, t) \log u_{\alpha}(\mathbf{x}, t) d\mathbf{x} = - \sum_{\alpha=1}^N \int_{\mathbb{R}^n} p_{\alpha}(\mathbf{x}, t) \log [\lambda_{\alpha} p_{\alpha}(\mathbf{x}, t)] d\mathbf{x} \quad (30)$$

where  $u_{\alpha}(\mathbf{x}, t)$  are defined by eq. (22). From the evolution equations (23) it follows after some algebra that

$$\frac{d\hat{S}_{BS}(t)}{dt} = (\mathbf{u}, \log \mathbf{u})_{L_N^2} - (\mathbf{A}\mathbf{u}, \log \mathbf{u})_{L_N^2} \quad (31)$$

where we have used the notation  $\mathbf{u} = (u_1, \dots, u_N)$ ,  $\log \mathbf{u} = (\log u_1, \dots, \log u_N)$ . Eq. (31) is formally analogous to a previously treated case, see eq. (19), so that

$$\frac{d\hat{S}_{BS}(t)}{dt} = \int_{\mathbb{R}^n} r_S(u(\mathbf{x}, t)) d\mathbf{x} \quad (32)$$

where

$$r_S(\mathbf{u}) = \frac{1}{2} \sum_{\alpha, \gamma=1}^N A_{\alpha, \gamma} (u_{\alpha} - u_{\gamma}) \log \left( \frac{u_{\alpha}}{u_{\gamma}} \right) \geq 0 \quad (33)$$

### 2.3 A simple example

This paragraph highlights the dissipation properties addressed in the previous paragraph through a simple example. Consider the one-dimensional, purely stochastic ( $v(x) = 0$ ) Poisson-Kac process  $dx(t) = b(-1)^{\chi(t)} dt$  on the unit interval with reflective conditions at the boundaries. Keeping fixed

$D_{\text{eff}} = b^2/2\lambda = 1$ , use the transition rate  $\lambda$  as a parameter. As initial condition take

$$p^+(x, 0) = p^-(x, 0) = \begin{cases} 1/4d & |x - 1/2| \leq 0 \\ 0 & \text{otherwise} \end{cases} \quad (34)$$

so that  $\int_0^1 p(x, t) dx = 1$  for  $t \geq 0$ . The energy dissipation function introduced in the previous paragraph can be normalized by considering the auxiliary function

$$\mathcal{E}_d^*(t) = 2\mathcal{E}_d(t) - \frac{1}{2} \quad (35)$$

so that  $\lim_{t \rightarrow \infty} \mathcal{E}_d^*(t) = 0$ . The Fickian counterpart of  $\mathcal{E}^*(t)$  is represented by

$$E^*(t) = \int_0^1 p^2(x, t) dx - 1 = \|p - 1\|_{L^2}^2 \quad (36)$$

that corresponds to the square of the  $L^2$ -norm of the overall probability density function normalized to zero mean. Figure 1 depicts several concentration profiles of the overall probability density function  $p(x, t)$  for  $\lambda = 10$ , sampled at time-intervals of 0.1, just to visualize the typical deviation from Brownian evolution characterizing Poisson-Kac dynamics at short timescales.

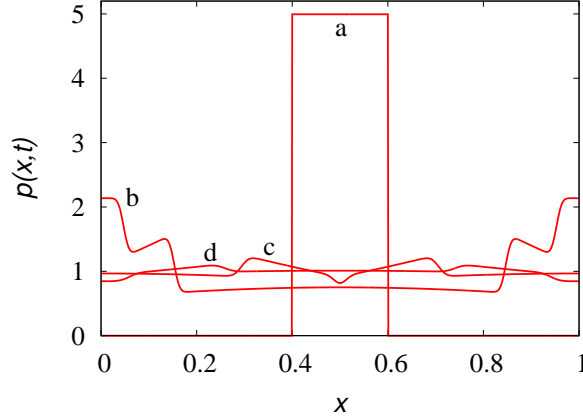


Figure 1:  $p(x, t)$  vs  $x$  at several time instant for  $\lambda = 10$ . Line (a) refers to the initial condition (34), line (b) to  $t = 0.1$ , line (c) to  $t = 0.2$ , line (d) to  $t = 0.3$ .

The comparison between the Fickian  $E^*(t)$  and the correct  $\mathcal{E}_d^*(t)$  energy dissipation functions is depicted in panels (a) and (b) of figure 2. While  $E^*(t)$  exhibits an evident non-monotonic behavior as a function of  $t$  in the range of transition rates  $\lambda \in (0.1, 10)$ , that becomes more pronounced as  $\lambda$  decreases, the function  $\mathcal{E}_d^*(t)$  is monotonically non-increasing. This example

expresses pictorially the claim that an energy-dissipation function which is a quadratic functional solely of the overall probability density cannot be compatible with Poisson-Kac dynamics, and more generally with stochastic evolution possessing a finite propagation velocity. Conversely, the function  $\mathcal{E}_d^*(t)$ , that depends on the whole system of partial waves - in the present case  $p^+(x, t)$  and  $p^-(x, t)$  - provides a correct description of dissipation. This example supports the fundamental ansatz of the theory of extended thermodynamics that state and dissipation functions in irreversible processes should depend also on the fluxes, as  $\mathcal{E}_d^*(t)$  in the present case [3]. At  $\lambda = 100$  (lines (d))  $E^*(t)$  and  $\mathcal{E}_d^*(t)$  practically coincide, and this corresponds to the Kac limit of the process.

A specular behavior is displayed by the entropy function. In this framework, the behavior of the Boltzmann-Shannon entropy  $S_{BS}(t)$  based on the full structure of the partial probability waves should be contrasted with the classical Boltzmannian entropy  $\Sigma_B(t)$

$$\Sigma_B(t) = - \int_0^1 p(x, t) \log p(x, t) dx \quad (37)$$

depending exclusively on the overall probability density function  $p(x, t)$ . Panel (c) and (d) of figure 2 show the comparison of these two entropy functions. A similar analysis based on the Cattaneo equation has been performed by Jou et al. [3]. All the observations addressed for the energy dissipation functions apply *verbatim* to  $\Sigma_B(t)$  and  $S_{BS}(t)$ . In the long-term limit  $\Sigma_B(t) \rightarrow 0$ , while  $S_{BS}(t) \rightarrow \log 2$ , corresponding to the complete homogenization amongst the partial waves.

## 2.4 Relativistic transformation of entropy

At the end of paragraph 2.2 the expression for the entropy of a GPK process possessing a symmetric transition probability matrix and generic transition rates has been obtained, eq. (30). This case find application in relativistic analysis of stochastic processes as outlined below.

Consider a one-dimensional, purely diffusive Poisson-Kac dynamics in an inertial reference frame  $\Sigma$ , defined by the space-time coordinates  $(x, t)$ ,  $dx(t) = b(-1)^{\chi(t)} dt$ , in which the evolution equations of the partial probability waves of the process  $p^\pm(x, t)$  is expressed by eq. (1). The frame  $\Sigma$  can be referred to as the *rest frame* of the process, since the process is characterized by a vanishing effective velocity (corresponding to the time-derivative of the first-order moment in the long-term regime).

Let  $\Sigma'$  be another inertial frame, defined by the space-time coordinates  $(x', t')$  moving with respect to  $\Sigma$  at constant relative velocity  $v < c$ , where  $c$  is the velocity of light *in vacuo*. Enforcing the Lorentz boost connecting

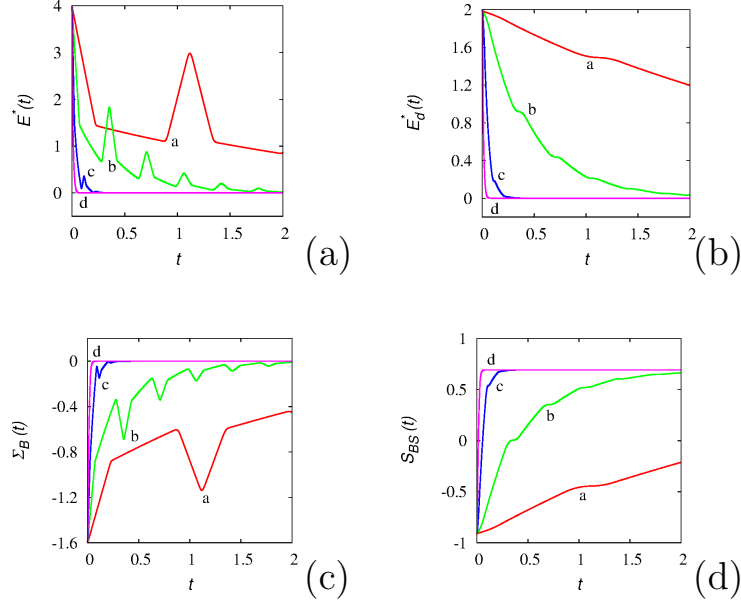


Figure 2: Review of the time evolution of dissipation and entropy functions for the Poisson-Kac process considered in the main text at  $D_{\text{eff}} = 1$ . Panel (a) refers to  $E^*(t)$ , panel (b) by to  $\mathcal{E}_d^*(t)$ , panel (c) to the Boltzmannian entropy  $\Sigma_B(t)$ , panel (d) to the Boltzmann-Shannon entropy  $S_{BS}(t)$  defined using the partial probability waves. Lines from (a) to (d) in all the panels refer to  $\lambda = 0.1, 1, 10, 100$ , respectively.

$(ct', x')$  to  $(ct, x)$ ,

$$\begin{pmatrix} ct' \\ x' \end{pmatrix} = \gamma(v) \begin{pmatrix} 1 & -\beta \\ -\beta & 0 \end{pmatrix} \begin{pmatrix} ct \\ x \end{pmatrix} \quad (38)$$

where  $\gamma(v) = 1/\sqrt{1 - v^2/c^2}$  is the Lorentz factor and  $\beta = v/c$ , the statistical description of the process in  $\Sigma'$  involves the partial probability density functions  $p^{\pm, \prime}(x', t')$  that satisfy the balance equations [16, 17]

$$\begin{aligned} \partial_{t'} p^{+, \prime}(x', t') &= -b'_+ \partial_{x'} p^{+, \prime}(x', t') - \lambda'_+ p^{+, \prime}(x', t') + \lambda'_- p^{-, \prime}(x', t') \\ \partial_{t'} p^{-, \prime}(x', t') &= -b'_- \partial_{x'} p^{-, \prime}(x', t') + \lambda'_+ p^{+, \prime}(x', t') - \lambda'_- p^{-, \prime}(x', t') \end{aligned} \quad (39)$$

where the velocities  $b'_\pm$  satisfy the usual relativistic velocity transformation for  $b$  and  $-b$ , respectively,

$$b'_+ = \frac{b - v}{1 - bv/c^2}, \quad b'_- = \frac{-b - v}{1 + bv/c^2} \quad (40)$$

while the transition rates  $\lambda'_\pm$  in  $\Sigma'$  are expressed by the relations (see [16, 17])

$$\lambda'_+ = \frac{\lambda}{\gamma(v)} \left(1 - \frac{bv}{c^2}\right)^{-1}, \quad \lambda'_- = \frac{\lambda}{\gamma(v)} \left(1 + \frac{bv}{c^2}\right)^{-1} \quad (41)$$

The Lorentz boost does not change the transition probability matrix, that in the present case is  $\mathbf{A}' = \mathbf{A} = \begin{pmatrix} 0 & 1 \\ 1 & 0 \end{pmatrix}$ , but modifies the transition rates  $\lambda'_+$ ,  $\lambda'_-$  in  $\Sigma'$ . The transition rates  $\lambda_+$ ,  $\lambda_-$  coincide at  $v = 0$  but, as the velocity  $v$  increases, become progressively more different from each other. In  $\Sigma'$  the stochastic process considered is still a GPK process with uneven transition rates and symmetric transition probability matrix, as addressed at the end of paragraph 2.2. Consequently, a suitable expression for the entropy function in a generic frame is given by eq. (30), i.e.

$$\widehat{S}_{BS}(t) = - \int_{-\infty}^{\infty} [p^+(x, t) \log(\lambda_+ p^+(x, t)) + p^-(x, t) \log(\lambda_- p^-(x, t))] dx \quad (42)$$

In  $\Sigma$ ,  $\lambda_+ = \lambda_- = \lambda$  and eq. (42) returns

$$\widehat{S}_{BS}(t) = - \int_{-\infty}^{\infty} [p^+(x, t) \log p^+(x, t) + p^-(x, t) \log p^-(x, t)] dx - \log \lambda = S_{BS}(t) - \log \lambda \quad (43)$$

while in  $\Sigma'$ , the entropy function becomes

$$\widehat{S}'_{BS}(t') = - \int_{-\infty}^{\infty} [p^{+'}(x', t') \log(\lambda'_+ p^{+'}(x', t')) + p^{-'}(x', t') \log(\lambda'_- p^{-'}(x', t'))] dx' \quad (44)$$

Set  $c = 1$  a.u., and  $b = c$ , i.e., consider a stochastic perturbation the characteristic velocity of which coincides with that of light, as for electromagnetic fluctuations. Figure 3 depicts the behavior of  $\widehat{S}'_{BS}(t')$  vs time  $t'$  for a Poisson-Kac process characterized in its rest frame by  $D_{\text{eff}} = 1$ , i.e.,  $\lambda = b^2/2D_{\text{eff}} = 1/2$ . The initial condition is symmetric and impulsive, namely  $p^+(x, 0) = p^-(x, 0) = \delta(x)/2$ , centered at the origin. Apart from the monotonic behavior of  $\widehat{S}'_{BS}(t')$  with time  $t'$ , it should be observed that the relativistic transformation of the modified Boltzmann-Shannon entropy cannot be easily expressed as a simple function of the Lorentz factor  $\gamma(v)$ , as occurs e.g. for the tensor diffusivity [16].

The extension to GPK processes is straightforward using the relativistic transformation for the partial probability densities developed in [17] and the results at the end of paragraph 2.2.

### 3 GPK processes and chaotic advection-diffusion problems

An interesting physical application of the GPK theory developed above involves tracer dynamics in chaotic flows in the presence of stochastic perturbations.

Consider a two-dimensional problem defined on the unit two-torus  $\mathcal{T}^2 = [0, 1] \times [0, 1]$ , equipped with periodic boundary conditions. Let  $\mathbf{v}(\mathbf{x}, t)$ ,  $\mathbf{x} =$

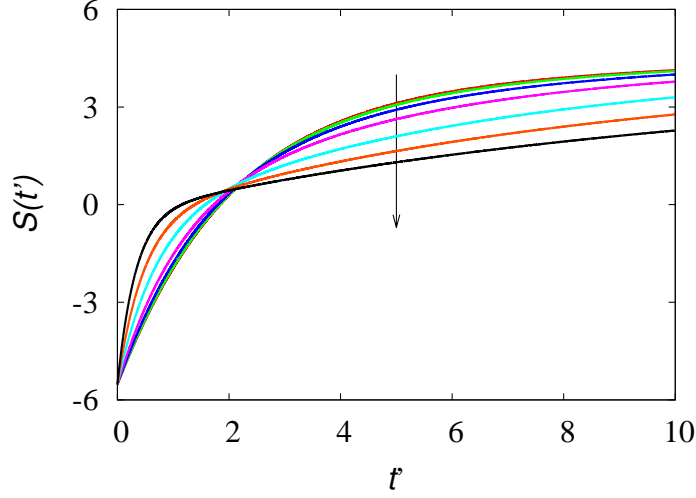


Figure 3:  $S(t') = \hat{S}'_{BS}(t')$  vs  $t'$  for the Poisson-Kac process on the real line measured in a reference system  $\Sigma'$  moving at constant relative velocity  $v$  with respect to the rest frame of the process. The arrow indicates increasing values of  $v = 0, 0.2, 0.4, 0.6, 0.8, 0.9, 0.95$ .

$(x, y)$  be a time-periodic solenoidal velocity field,  $\nabla \cdot \mathbf{v} = 0$ , and consider the GPK process

$$d\mathbf{x}(t) = \mathbf{v}(\mathbf{x}(t), t) dt + \frac{1}{Pe} \mathbf{b}_{\chi_N(t)} dt \quad (45)$$

Equation (45) represents the dimensionless kinematic equations of motion of a passive tracer in an incompressible flow subjected to stochastic (thermal) agitation expressed by a finite  $N$ -state Poisson process acting on a family of  $N$  stochastic velocity vectors. The parameter  $Pe$  is the Péclet number, representing the ratio of the characteristic diffusion to the characteristic advection times.

Assume for the  $N$ -state finite Poisson process a constant transition rate  $\lambda$ , and a transition probability matrix expressed by  $A_{\alpha, \beta} = 1/N$ ,  $\alpha, \beta = 1, \dots, N$ . For the stochastic velocity vectors  $\mathbf{b}_\alpha$  choose the family given by eq. (78) in part I, so that  $D_{\text{nom}} = 1$ . As regards the velocity field, consider a simple but widely used model of Hamiltonian chaos, originating from the standard map  $\mathbf{x}' = \Phi(\mathbf{x})$  [7, 8], expressed by

$$\begin{cases} x' = x + \frac{\nu}{2\pi} \sin(2\pi y) & \text{mod. } 1 \\ y' = y + x' & \text{mod. } 1 \end{cases} \quad (46)$$

where  $\nu > 0$  is a real parameter. In a continuous time setting, the standard map can be recovered as the stroboscopic map associated with the time-

periodic incompressible flow possessing period  $T = 2$  obtained from the periodic repetition of the flow protocol

$$\mathbf{v}(\mathbf{x}, t) = \begin{cases} (\frac{\nu}{2\pi} \sin(2\pi y), 0) & 0 \leq t < 1 \\ (0, x) & 1 \leq t < 2 \end{cases} \quad (47)$$

and corresponding to the periodic switching of two shear flows along the  $x$ - and  $y$ -coordinates, respectively, the first of which is sinusoidally modulated. Observe that the second flow, is not continuous on the torus, while the resulting stroboscopic map is  $C^\infty$ .

By varying the parameter  $\nu$ , the typical phenomenologies of chaotic advection can be recovered from the standard map. We consider the case  $\nu = 1$ , the Poincaré map of which (i.e., the stroboscopic map sampled at the period of the flow protocol) is depicted in figure 4, and is characterized by the presence of invariant chaotic regions possessing a maximum positive Lyapunov exponent, intertwined with regular invariant islands of different sizes.

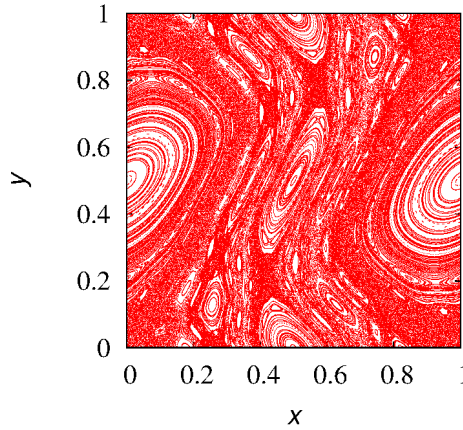


Figure 4: Poincaré map of the standard map at  $\nu = 1$ .

In the Kac limit, the statistical characterization of eq. (45) converges to the solution of a classical parabolic advection-diffusion equation for the overall probability density function  $p(\mathbf{x}, t)$ ,

$$\partial_t p(\mathbf{x}, t) = -\mathbf{v}(\mathbf{x}, t) \cdot \nabla p(\mathbf{x}, t) + \frac{1}{Pe} \nabla^2 p(\mathbf{x}, t) \quad (48)$$

Consider as an initial condition a completely segregated initial profile of the partial probability waves, namely

$$p_\alpha(\mathbf{x}, 0) = \begin{cases} 2/N & 0 \leq x < 1/2 \\ 0 & 1/2 \leq x < 1 \end{cases} \quad \alpha = 1, \dots, N \quad (49)$$

and let  $E^*(t)$  be the normalized  $L^2$ -norm of  $p(\mathbf{x}, t)$

$$E^*(t) = \frac{\|p(\mathbf{x}, t) - 1\|_{L^2}}{\|p(\mathbf{x}, 0) - 1\|_{L^2}} \quad (50)$$

so that  $E^*(0) = 1$  and  $\lim_{t \rightarrow \infty} E^*(t) = 0$ .

Figure 5 depicts the evolution of  $E^*(t)$  and at two different values of the Péclet number:  $Pe = 10^1$  (panel a) and  $Pe = 10^2$  (panel b). Numerical simulations have been performed by expanding  $p_\alpha(\mathbf{x}, t)$  in truncated Fourier series,  $p_\alpha(\mathbf{x}, t) = \sum_{h,k=-N_c}^{N_c} P_{\alpha,h,k} e^{i2\pi(hx+ky)}$ , solving the corresponding system of linear differential equations for the Fourier coefficients  $P_{\alpha,h,k}$  with an explicit 4-th order Runge-Kutta solver. For the range of  $Pe$  values considered  $Pe \leq 10^2$ , we choose  $N_c = 50$ , which is fully sufficient for an accurate description of the dynamics, apart from the very early stages of the process. These graphs refer to a GPK process with  $N = 4$  using the transition rate  $\lambda$  as parameter. The case  $Pe = 10^1$  (panel a) is indicative of the typical relaxation properties of GPK systems: the normalized  $L^2$ -norm  $E^*(t)$  decays asymptotically in an exponential way  $E^*(t) \sim e^{-\mu(\lambda)t}$ , but for moderate values of  $\lambda$ , the decay exponent  $\mu(\lambda)$  is a function of the transition rate  $\lambda$  and is smaller than the limit value  $\mu_\infty = \lim_{\lambda \rightarrow \infty} \mu(\lambda)$ .

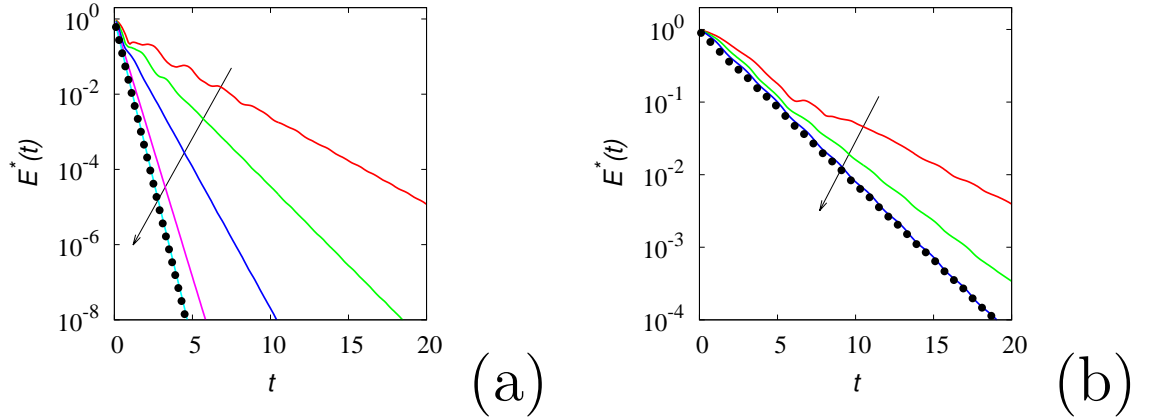


Figure 5: Normalized square  $L^2$ -norm  $E^*(t)$  vs time  $t$  for the GPK flow associated with the standard map ( $N = 4$ ) at  $Pe = 10^1$  (panel a), and  $Pe = 10^2$  (panel b). Symbols ( $\bullet$ ) represent the solution of the corresponding parabolic advection-diffusion equation (48). The arrows indicate increasing values of  $\lambda$ . Panel (a):  $\lambda = 0.5, 1, 2, 4, 10, 40$ . Panel (b):  $\lambda = 0.5, 1, 2$ .

As  $\lambda$  increases, the Kac-limit property dictates that  $\mu(\lambda)$  converges towards the decay exponent  $\Lambda(Pe)$  of the parabolic advection-diffusion model (48) for the same value of the Péclet number, i.e.  $\mu_\infty = \Lambda(Pe)$ . The



convergence of  $\mu(\lambda)$  towards  $\mu_\infty$  is depicted in figure 6, plotting the ratio  $r_\mu(\lambda) = [\mu_\infty - \mu(\lambda)]/\mu_\infty$  vs  $\lambda$  for the two Péclet values considered. At  $Pe = 10^1$ , the Kac convergence is achieved approximately for  $\lambda \geq 10^2$ . At higher Péclet values, the influence of  $\lambda$  is less pronounced and the Kac-limit convergence is practically achieved at smaller values of  $\lambda$ , e.g.  $\lambda \geq 2$  for  $Pe = 10^2$ .

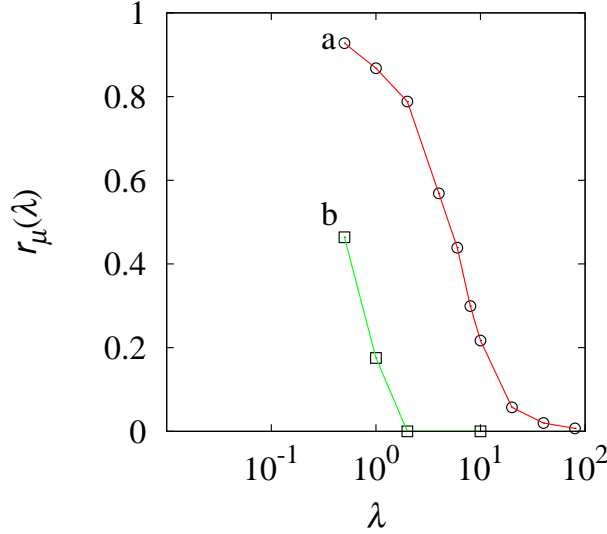


Figure 6: Ratio  $r_\mu(\lambda) = [\mu_\infty - \mu(\lambda)]/\mu_\infty$  vs  $\lambda$  for the standard-map flow considered in the main text. Line (a) and (o) refers to  $Pe = 10^1$ , line (b) and ( $\square$ ) to  $Pe = 10^2$ .

Figure 7 depicts a review of the early-time dynamics, at four time instants  $t = nT$ ,  $n = 1, 2, 3, 10$ , at  $Pe = 10^2$ , referred to the contour plots of the rescaled overall probability density profiles  $p^*(\mathbf{x}, t) = C(p(\mathbf{x}, t) - 1)$ , where  $C$  is a normalization constant so that  $p^*(\mathbf{x}, t)$  possess unit  $L^2$ -norm. Two situations are considered: far way from the Kac limit ( $\lambda = 1$ ), panels (a)-(d), and close to the Kac limit ( $\lambda = 10$ ), panels (a')-(d'), compared to the corresponding profiles obtained from the solution of the parabolic advection-diffusion equation (48), panel (a\*), (d\*). The probability density profiles at  $\lambda = 1$  still show a significant effect of the hyperbolic (undulatory) dynamics characterizing the evolution of the partial probability waves, as the density profiles display much sharper discontinuities with respect to the smoother behavior displayed by the solutions of the parabolic equation (48). The graph for  $t = nT = 20$  depicted in the last row correspond to the profile in asymptotic conditions of the second eigenfunction of the Floquet operator associated with the advection-diffusion dynamics, see [18].

Next, consider the energy dissipation functions and entropies. A review

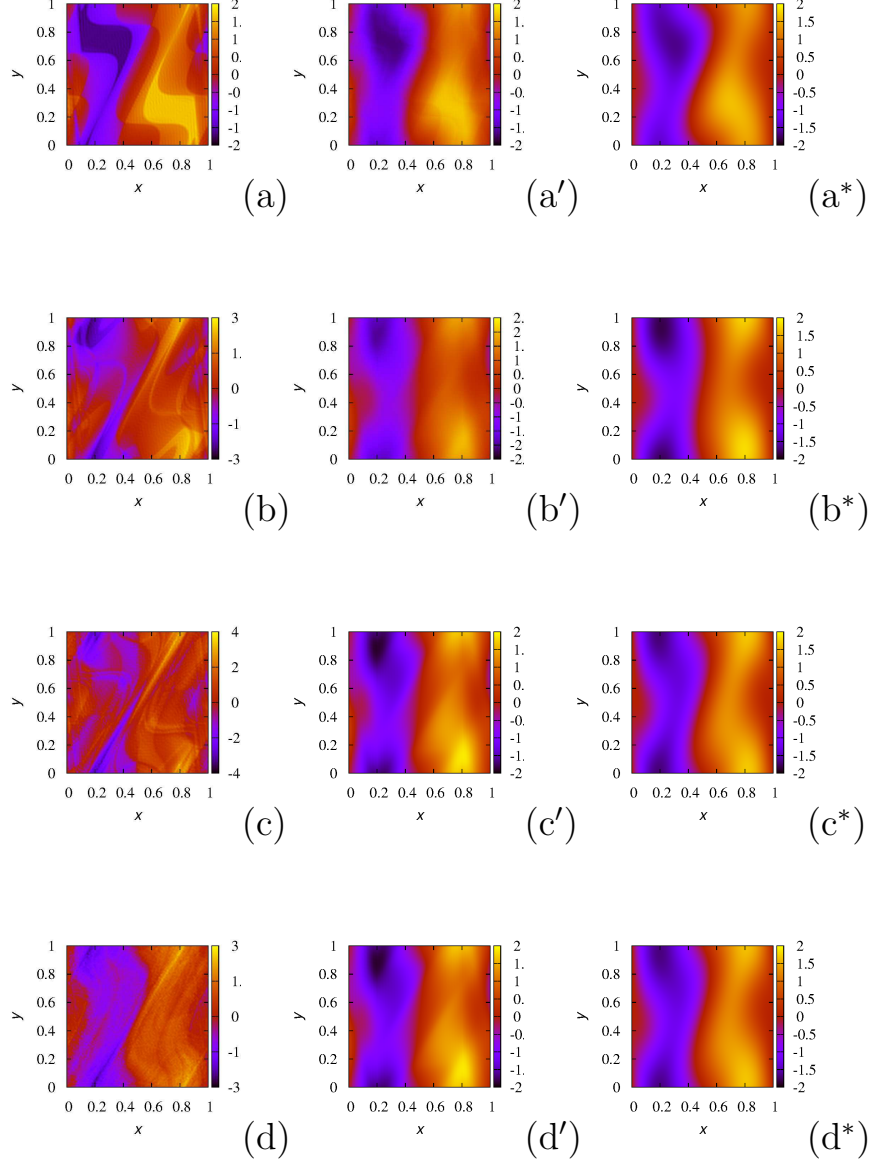


Figure 7: Concentration profiles of  $p^*(\mathbf{x}, t)$  at  $Pe = 10^2$ ,  $N = 4$  at  $t = nT$ . Upper row  $n = 1$ , second row  $n = 2$ , third row  $n = 3$ , and lower row  $n = 10$ . Panels (a)-(d), first column, refer to  $\lambda = 1$  panels (a')-(d'), second column, to  $\lambda = 10$ ; panels (a\*)-(d\*), third column, to the solution of the parabolic advection-diffusion equation (48).

of their behavior at  $Pe = 10^1$ ,  $\lambda = 1$  is depicted in figure 8, panels (a) to (d), using the number  $N$  of stochastic velocity vectors as parameter. In

these plots,  $E_d^*(t)$  is the normalized energy dissipation function based on the partial probability waves expressed as

$$E_d^*(t) = \frac{\mathcal{E}_d^*(t)}{\mathcal{E}_d^*(0)} \quad \mathcal{E}_d^*(t) = \frac{1}{2} \sum_{\alpha=1}^N \left\| p_{\alpha}(\mathbf{x}, t) - \frac{1}{N} \right\|_{L^2} \quad (51)$$

while the normalized Boltzmann-Shannon entropy  $S_{BS}^*(t)$  is the difference between the Boltzmann-Shannon entropy  $S_{BS}(t)$  and its limit value  $\log N$  for  $t \rightarrow \infty$ ,

$$S_{BS}^*(t) = S_{BS}(t) - \log N \quad (52)$$

so that  $\lim_{t \rightarrow \infty} S_{BS}^*(t) = 0$  as for the Boltzmannian entropy  $\Sigma_B(t)$ .

The comparisons of  $E^*(t)$  and  $E_d^*(t)$  (panels (a) and (b)) and of  $\Sigma_B(t)$  and  $S_{BS}^*(t)$  (panels (c) and (d)) indicate that the dissipation functionals  $E^*(t)$  and  $\Sigma_B(t)$  based exclusively on the overall probability density function  $p(\mathbf{x}, t)$  display a non-monotonic/oscillatory behavior, while the corresponding quantities  $E_d^*(t)$  and  $S_{BS}^*(t)$  based on the full structure of the partial probability waves are monotonic functions of time  $t$ . This is analogous to the case of the purely diffusive one-dimensional Poisson-Kac model addressed in paragraph 2.3. There is however, a major conceptual difference between the two problems, as regard the representation of the dissipation functions. In the one-dimensional problem treated in paragraph 2.3,  $p^+(x, t)$  and  $p^-(x, t)$  can be expressed as a linear combination of  $p(x, t)$  and  $J_d(x, t)$ ,  $p^{\pm}(x, t) = [p(x, t) \pm J_d(x, t)] / 2$ , indicating that, in the one-dimensional case in the presence of the two-state process  $(-1)^{\chi(t)}$ , a correct energy dissipation function and a consistent expression for the entropy can be always expressed in terms of the overall probability density function  $p(x, t)$  and of its diffusive flux  $J_d(x, t)$ .

This functional symmetry is broken in the two-dimensional advection-diffusion problem considered in this paragraph whenever  $N \geq 4$ . For  $N \geq 4$ , the functional expressions for  $E_d^*(t)$  and  $S_{BS}^*(t)$  cannot be expressed exclusively in terms of  $p(\mathbf{x}, t)$  and  $\mathbf{J}_d(\mathbf{x}, t)$  as they depend on the complete statistical structure of the GPK process, which is accounted for by the system of partial probability waves  $\{p_{\alpha}(\mathbf{x}, t)\}_{\alpha=1}^N$ .

This is a first, physically significant, case in which the concentration/flux paradigm characterizing the classical theory of transport phenomena [19] results insufficient. There is a further observation emerging from the analysis of the data depicted in figure 8. The decay dynamics of the energy dissipation functions and entropies depend on the number  $N$  of stochastic velocity vectors considered. However, as  $N$  increases, a limit behavior occurs, indicating that, above a given threshold  $N^*$ , the use of a higher number  $N > N^*$  of states (velocity vectors) is practically immaterial.

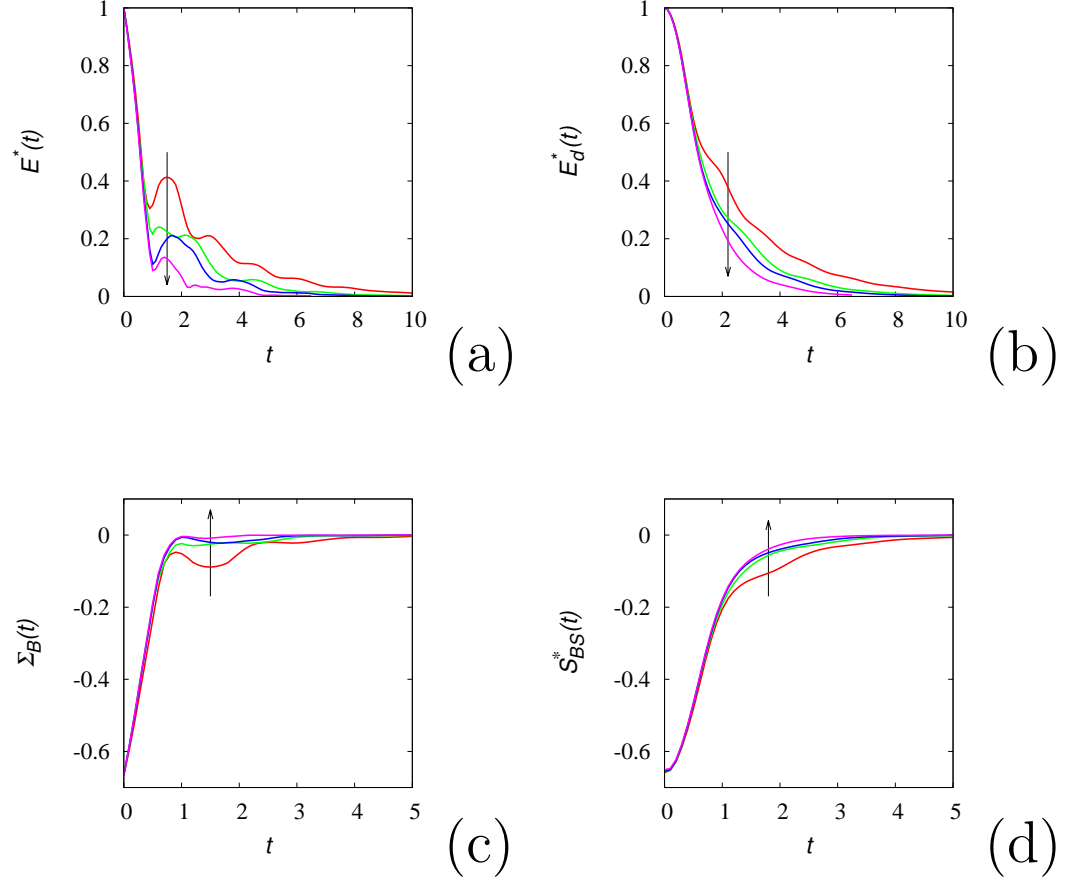


Figure 8: Review of the energy-dissipation functions/entropies for the GPK processes associated with the standard-map flow at  $Pe = 10^1$ ,  $\lambda = 1$ . The arrows in the four panels indicate increasing values of  $N = 3, 4, 5, 10$ . Panels (a)-(b) depict energy-dissipation functions: panel (a) refers to  $E^*(t)$  vs  $t$ , panel (b) to  $E_d^*(t)$  vs  $t$ . Panels (c)-(d) depict entropy functions: panel (c) refers to the Boltzmannian entropy  $\Sigma_B(t)$  vs  $t$ , panel (d) to the rescaled entropy  $S_{BS}^*(t)$  based on the full structure of the partial probability waves  $\{p_\alpha(\mathbf{x}, t)\}_{\alpha=1}^N$ .

## 4 Physical properties

In this Section, we address some physical observations on the properties of GPK processes that can be of interest in several branches of physics.

## 4.1 Stochastic field equations and Brownian-motion mollification

Starting from the works by Wong and Zakai [20, 21], mollification (regularization) of Wiener processes and Wiener-driven stochastic differential equations has become an important field of stochastic analysis. In the original Wong-Zakai papers, Wiener processes have been mollified using interpolation techniques obtaining piecewise linear, and therefore almost everywhere (a.e.) smooth approximations of Brownian motion. The so-called Wong-Zakai theorem derived by these authors admits several important implications in stochastic theory [22, 23, 24] and the mollified version of a Langevin equation is described statistically in a suitable limit by the Stratonovich Fokker-Planck equation associated with the original Langevin model, using the Stratonovich recipe for the stochastic integrals.

Poisson-Kac and GPK processes provide a physically significant way of mollifying stochastic dynamics, as the Poisson-Kac perturbations, admitting a finite propagation velocity, evolves as a physical field, and possess a.e. regular trajectories. This property is particularly important in all the cases, the stochastic perturbation does not derive by a coarse-grained approximation of many uncorrelated disturbances, but admits itself a fundamental physical nature, such as the fluctuating component of the electromagnetic field (including the zero-point field), which plays a central role in quantum electrodynamics, in understanding fundamental particle-field interactions, and in general cosmology [25].

In this framework, GPK processes are the natural candidates for attempting a modeling of fundamental field fluctuations, since their wave-like propagation intrinsically match the requirement of special relativity as it regards the bounds on the propagation velocity. It is rather straightforward to derive from Poisson-Kac and GPK processes a Wong-Zakai theorem connecting the Kac limit to the Stratonovich Fokker-Planck equation.

Mollification of Brownian motion can be of wide mathematical physical interest in connection with the analysis of Stochastic Partial Differential Equation (SPDE), that recently experienced significant progresses due to the introduction of new concept and mathematical tools such as that of “regularity structures” and rough-path analysis [26, 27].

For SPDE and in stochastic field theory, the use of Poisson-Kac and GPK processes provides an interesting alternative approach in order to study these models using a.e. differentiable stochastic perturbations (which are definitely simpler to handle both numerically and theoretically), and considering their Kac limit for approaching the nowhere-differentiable case.

Let us clarify this approach with a very simple example, leaving the analysis of physically interesting SPDE to future works. Let  $\Omega$  be a bounded domain of  $\mathbb{R}^n$  and  $\mathcal{L} : \mathcal{D}(\Omega) \rightarrow L^2(\Omega)$  a differentiable operator, mapping a subset  $\mathcal{D}(\Omega) \subset L^2(\Omega)$  into  $L^2(\Omega)$ , equipped with suitable boundary condi-

tions at  $\partial\Omega$ . Assume that  $\mathcal{L}$ , equipped with the given boundary conditions, admit a complete eigenbasis  $\{\psi_k(\mathbf{x})\}_{k=1}^{\infty}$

$$\mathcal{L}[\psi_k(\mathbf{x})] = \mu_k \psi_k(\mathbf{x}) \quad (53)$$

normalized to unit  $L^2$ -norm, spanning  $L^2(\Omega)$ . The simplest case is  $\mathcal{L} = \nabla^2$  equipped at the boundary of the domain, say with homogeneous Dirichlet conditions.

Let us consider a linear SPDE, given by

$$\partial_t c(\mathbf{x}, t) = \mathcal{L}[c(\mathbf{x}, t)] + b(\mathbf{x}) (-1)^{\chi(t)} \quad (54)$$

where  $\chi(t)$  is a simple Poisson process characterized by the transition rate  $\lambda$ . If  $\mathcal{L} = \nabla^2$ , eq. (54) is a modified form of the Edwards-Wilkinson model [28, 29] of interface dynamics. Setting  $c(x, t) = \sum_{k=1}^{\infty} c_k(t) \psi_k(\mathbf{x})$ , eq. (54) reduces to the system of stochastic differential equations for the Fourier coefficients

$$dc_k(t) = \mu_k c_k(t) dt + b_k (-1)^{\chi(t)} dt \quad (55)$$

where  $b_k = \int_{\Omega} b(\mathbf{x}) \psi_k(\mathbf{x}) d\mathbf{x}$ . The evolution equations for the associated partial waves  $p^{\pm}(\{c_k\}_{k=1}^{\infty}, t)$  thus become

$$\partial_t p^{\pm} = - \sum_{k=1}^{\infty} \partial_k [(\mu_k c_k \pm b_k) p^{\pm}] \mp \lambda (p^{+} - p^{-}) \quad (56)$$

that can be solved truncating the summation up to a given integer  $N$ . From eq. (56) all the information on the mean field

$$\langle c(\mathbf{x}, t) \rangle = \sum_{k=1}^{\infty} \psi_k(\mathbf{x}) \int c_k p(\{c_k\}_{k=1}^{\infty}, t) d\mathbf{c} \quad (57)$$

where  $d\mathbf{c} = \prod_{k=1}^{\infty} dc_k$ , as well as on the correlation functions can be derived.

The problem analyzed above is fairly simple as the noise perturbation does not depend on  $\mathbf{x}$ . It is however straightforward to consider space-time Poisson processes representing mollifications of delta-correlated stochastic perturbations both in time and in space, which is the classical prototype of stochastic forcing in many problems involving SPDE.

Consider for example a one-dimensional space dimension. Since the spatial coordinate is defined also for negative values, the extension of a Poisson-Kac process over the real line is necessary. This can be performed, as for the Wiener case, by considering two independent Poisson processes  $\chi_{1'}(x)$  and  $\chi_{1''}(x)$ , possessing the same transition rate  $\lambda_1$ , and defined for  $x \geq 0$ , by introducing the extended process  $\chi_1(x)$  defined for  $x \in \mathbb{R}$  as

$$\chi_1(x) = \begin{cases} \chi_{1'}(-x) & x < 0 \\ \chi_{1''}(x) & x > 0 \end{cases} \quad (58)$$

Next consider process  $\chi(x, t)$ ,  $(x, t) \in \mathbb{R} \times \mathbb{R}^+ + \{0\}$  defined as

$$\chi(x, t) = \chi_1(x) + \chi_2(t) \quad (59)$$

where  $\chi_1(x)$  and  $\chi_2(t)$  are two independent Poisson processes characterized by transition rates  $\lambda_1$  and  $\lambda_2$ , respectively, where  $\chi_1(x)$  is the extended process defined by eq. (58), and the SPDE

$$\partial_t c(x, t) = \mathcal{L}[c(x, t)] + \alpha b(x) (-1)^{\chi(x, t)} \quad (60)$$

$x \in \mathbb{R}$ , where  $\alpha > 0$  is a parameter specified below. As regards the correlation properties of the noise perturbation one has

$$\begin{aligned} \left\langle (-1)^{\chi(x', t')} (-1)^{\chi(x, t)} \right\rangle &= \left\langle (-1)^{\chi_1(x') - \chi_1(x)} (-1)^{\chi_2(t') - \chi_2(t)} \right\rangle \\ &= e^{-2\lambda_1 |x' - x|} e^{-2\lambda_2 |t' - t|} \end{aligned} \quad (61)$$

Therefore, if one sets  $\alpha$  equal to

$$\alpha = \sqrt{4\lambda_1 \lambda_2} \quad (62)$$

the process  $\alpha (-1)^{\chi(x, t)}$  corresponds to a mollification of a  $\delta$ -correlated process both in time and space, converging to it in the limit  $\lambda_1, \lambda_2 \rightarrow \infty$ .

The evolution equations for the Fourier coefficients of  $c(x, t)$  become

$$dc_k(t) = \mu_k c_k(t) dt + \alpha b_k (-1)^{\chi_2(t)} dt \quad (63)$$

where

$$b_k = \int_{-\infty}^{\infty} (-1)^{\chi_1(x)} b(x) \psi_k(x) dx \quad (64)$$

The expression for the random variables  $b_k$  can be easily obtained by considering the dichotomous nature of  $(-1)^{\chi_1(x)}$ , and the fact that the transition instants follows an exponential distribution defined by the transition rate  $\lambda_1$ .

In a similar way, nonlinear problems, as classical stochastic fluid dynamic models (e.g. Burgers equation), growth models (e.g. the KPZ equation), or the stochastic quantization of fields can be approached both numerically and theoretically. Once again, it is important to observe that the mollification arising from the use of Poisson-Kac and GPK process, is not just a mathematical artifact to regularize the structure of a SPDE, but a way of describing physical fluctuations possessing bounded propagation velocity, and intrinsic relativistic consistency. The extension to higher dimension is also straightforward, by considering space-time Poisson processes  $\chi(\mathbf{x}, t)$  in  $\mathbb{R}^n \times \mathbb{R}^+ + \{0\}$  defined, analogously to eq. (59) as  $\chi(\mathbf{x}, t) = \sum_{h=1}^n \chi_h(x_h) + \chi_{n+1}(t)$ .

## 4.2 Ergodicity and $L^2$ -dynamics

In this paragraph we address some issues on the ergodicity of Poisson-Kac and GPK processes and on some anomalies of  $L^2$ -dynamics in the presence of conservative deterministic fields, considering the one-dimensional Poisson-Kac process

$$dx(t) = v(x(t)) dt + b(-1)^{\chi(t)} dt \quad (65)$$

$x \in \mathbb{R}$ . This paragraph represents a brief review with some extensions of the results presented in [11]. In one-dimensional problems,  $v(x)$  can be always regarded as a potential field deriving from the potential  $U(x) = -\int^x v(\xi) d\xi$ . The associated partial probability waves satisfy eqs. (A7) of part I where  $v_{\pm}(x) = v(x) \pm b$ . The stationary partial density functions  $p_{\pm}^{\pm}(x)$ , satisfy the differential equations

$$\begin{aligned} \frac{d(v_+(x)p_+^+(x))}{dx} &= -\lambda(p_+^+(x) - p_+^-(x)) \\ \frac{d(v_-(x)p_+^-(x))}{dx} &= \lambda(p_+^+(x) - p_+^-(x)) \end{aligned} \quad (66)$$

from which it follows that

$$v_+(x)p_+^+(x) + v_-(x)p_+^-(x) = C = \text{constant} \quad (67)$$

where the constant  $C$  should be in general equal to zero because of the regularity at infinity. Therefore,

$$p_+^-(x) = -\frac{v_+(x)}{v_-(x)} p_+^+(x) \quad (68)$$

Since by definition  $v^+(x) > v_-(x)$  for  $b > 0$ , it follows that a stationary (positive) partial probability density may occur solely within intervals  $(a, b)$ , where the conditions

$$v_-(x) < 0, \quad v_+(x) > 0 \quad x \in (a, b) \quad (69)$$

are satisfied. Conditions (69) correspond formally to the simultaneous presence of a forwardly propagating waves  $p^+(x, t)$  and of a backwardly propagating wave  $p^-(x, t)$ .

Suppose that  $v(x)$  and  $b$  are such that there exists a double sequence  $x_{-,h}^*, x_{+,h}$ ,  $h = -N_1, \dots, N_2$ ,  $N_1, N_2 > 0$ , of abscissas

$$\dots < x_{+,h-1}^* < x_{-,h}^* < x_{+,h}^* < x_{-,h+1}^* < \dots \quad (70)$$

such that  $\{x_{-,h}^*\}$  correspond to the nodal points of  $v_-(x)$ ,  $v_-(x_{-,h}^*) = 0$ , and  $\{x_{+,h}^*\}$  to the nodal point of  $v_+(x)$ ,  $v_+(x_{+,h}^*) = 0$ . From the above discussion, and from eq. (69), it follows that each subinterval  $I_h = [x_{-,h}^*, x_{+,h}^*]$  represents an invariant interval for the partial-wave dynamics. If more than



a single invariant interval exists, then the stochastic dynamics (65) is not ergodic, meaning that there exists a multiplicity of stationary invariant densities, each of which possesses compact support localized in the invariant intervals  $I_h$ .

A typical situation where invariant-density multiplicity occurs is depicted in figure 9 for a sinusoidal deterministic drift  $v(x) = \cos(x)$  and  $b < 1$  (actually  $b = 1/2$ ). The phenomenon of multiplicity of stationary invariant densities disappears generically for sufficiently large values of  $b$  and, *a fortiori*, in the Kac limit.

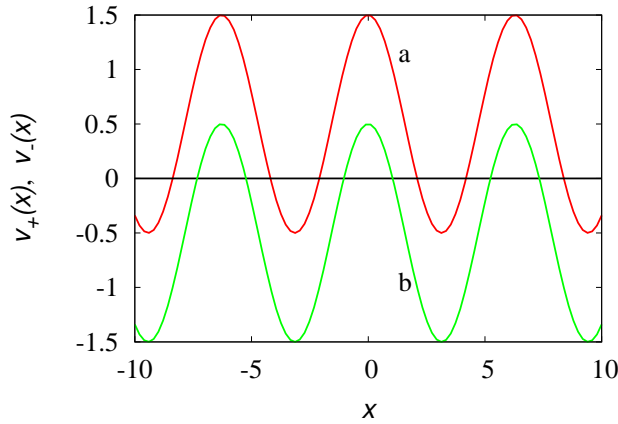


Figure 9:  $v_+(x)$  (line a) and  $v_-(x)$  (line b) for  $v(x) = \cos(x)$ ,  $b = 1/2$ .

There is another peculiarity of Poisson-Kac and GPK processes that should be addressed. In Section 2 we analyzed the property of energy dissipation functions represented by suitable  $L^2$ -norms of the partial probability density waves in two distinct cases: (i) in the absence of a deterministic bias, and (ii) where  $\mathbf{v}(\mathbf{x})$  is solenoidal i.e., it stems from a vector potential. The complementary case where  $\mathbf{v}(\mathbf{x})$  derives from a scalar potential, i.e.,  $\mathbf{v}(\mathbf{x}) = -\nabla\phi(\mathbf{x})$  has not been addressed. This was not fortuitous as, in the presence of potential velocity fields, the  $L^2$ -dynamics of the partial waves may display highly anomalous and singular properties for low values of the intensity of the stochastic velocity  $b$ . The archetype of such a singular behavior can be easily understood by mean of the one-dimensional model (65) defined on the unit interval  $[0, 1]$ , and equipped with reflecting conditions at the endpoints  $x = 0, 1$ . As a model of the deterministic bias  $v(x)$  choose, as an instance,

$$v(x) = \frac{3}{2} + \sin(2\pi x) \quad (71)$$

and take the stochastic velocity intensity  $b$  as a parameter. Figure 10 panel (a) depicts the behavior of  $v_{\pm}(x)$  at  $b = 0.7$ , while panel (b) refers to  $b =$

3/2. Let us analyze separately the two cases in terms of the qualitative

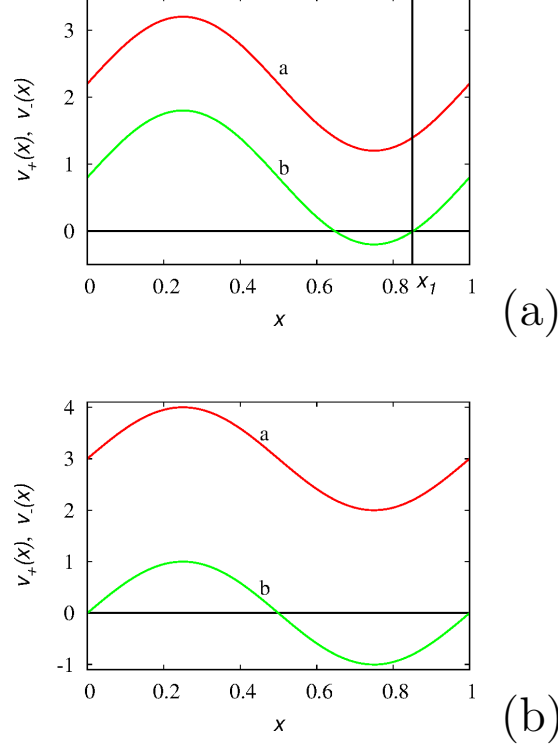


Figure 10:  $v_+(x)$  (line a) and  $v_-(x)$  (line b) for the deterministic field  $v(x)$  eq. (71) at two different values of  $b$ . panel (a):  $b = 0.7$ , panel (b);  $b = 3/2$ .

evolution of the partial probability waves. With reference to the case  $b = 0.7$  (panel a), the interval  $[0, x^*)$ , where  $x^*$  is the first zero of  $v_-(x)$ ,  $x^* \simeq 0.65$  is an escaping interval for the partial wave dynamics: both  $p^+(x, t)$  and  $p^-(x, t)$  are two progressive waves in  $[0, x^*)$ , so that there exists a time instant  $T^*$  such that, for  $t > T^*$  and for any initial condition,  $p^\pm(x, t) = 0$ ,  $x \in [0, x^*)$ . In the interval  $[x^*, x_1]$ , where  $x_1$  is the second zero of  $v_-(x)$  there is the coexistence of a forwardly propagating wave  $p^+(x, t)$ , and of a backwardly propagating one  $p^-(x, t)$ . Due to the recombination amongst the partial waves and to the fact that the forward  $p^+$ -wave propagates further towards  $x > x_1$ , even this subinterval will be eventually depleted, so that, for sufficiently long times  $t$ , both  $p^\pm(x, t)$  for  $x \in [x^*, x_1]$  will be arbitrarily small. Therefore, the wave-nature of the dynamics pushes the probability densities towards the interval  $(x_1, 1]$ . But in this region both  $v_\pm(x) > 0$  so that the two partial probability waves continue to propagate forward until they reach  $x = 1$  where they progressively accumulate due to the reflection conditions.

Therefore, just because of the reflecting boundary condition at  $x = 1$ , the unique stationary density becomes singular,

$$p_*^+(x) = p_*^-(x) = \frac{\delta(x-1)}{2} \quad (72)$$

Figure 11 depicts the evolution of the moments (panel a) and of the  $L^2$ -norms (panel b), obtained from stochastic simulations of eq. (65) at  $D_{\text{eff}} = 1$ , starting from an initial distribution localized at  $x = 0$ ,  $p^+(x, 0) = p^-(x, 0) = \delta(x)/2$ . As expected from eq. (72) the first-order moments  $m_1(t)$  approaches 1 at an exponential rate  $1 - m_1(t) \sim e^{-2\lambda t}$ . The variance  $\sigma_x^2(t)$  display a non-monotonic behavior with respect to  $t$ , converging asymptotically to zero at the same exponential rate.

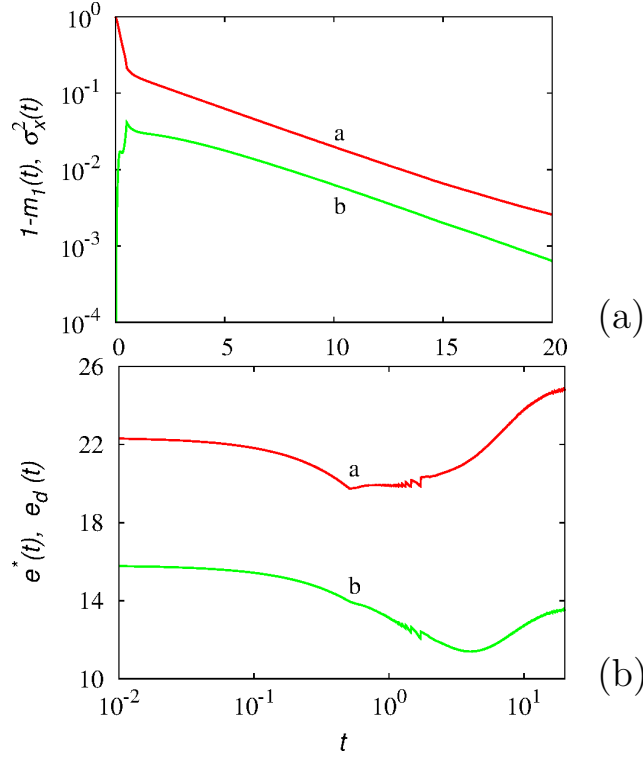


Figure 11: Panel (a):  $1 - m_1(t)$  (line a) and  $\sigma_x^2(t)$  (line b) for the model problem described in the main text at  $b = 0.7$ ,  $D_{\text{eff}} = 1$ . Panel (b): Norm dynamics for the same problem:  $e^*(t)$  (line a) and  $e_d(t)$  (line b) vs  $t$  (see the main text for the definition of these quantities).

As regards the  $L^2$ -norm depicted in panel (b), data have been obtained sampling a population of  $10^7$  particles using a partition of the unit interval into  $10^3$  subintervals. In this figure  $e^*(t) = \|p(x, t)\|_{L^2}$  and  $e_d(t) = \sqrt{\mathcal{E}_d(t)}$ ,

where  $\mathcal{E}_d(t) = (\|p^+(x, t)\|_{L^2}^2 + \|p^-(x, t)\|_{L^2}^2)/2$ . As expected, both these quantities admit a non-monotonic behavior and eventually diverge for  $t \rightarrow \infty$ .

The occurrence of a singular impulsive invariant density occurs for  $b < b^* = 3/2$  at which  $v_-(1) = 0$ . In this case,  $b = 3/2$ , a unique invariant density admitting compact non-atomic support in  $[x^*, 1]$ ,  $x^* = 1/2$  appears. From eqs. (66), (68), after elementary manipulations, the invariant density  $p_*(x)$  takes the expression

$$p_*(x) = \frac{A}{b^2 - v(x)} \exp \left[ -2\lambda \int_{x^*}^x \frac{v(\xi)}{v^2(\xi) - b^2} d\xi \right] \quad (73)$$

where  $A$  is a normalization constant.

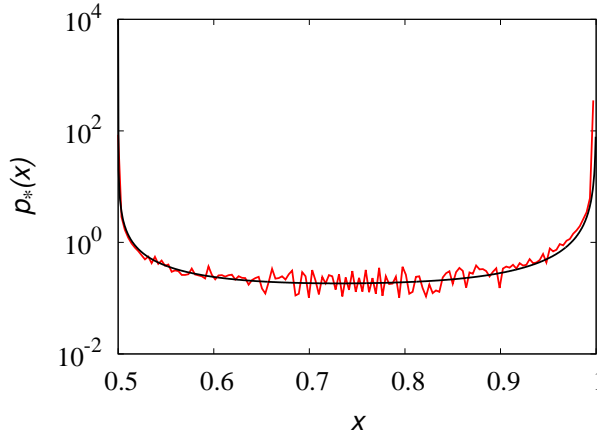


Figure 12: Invariant stationary probability density  $p_*(x)$  for the Poisson-Kac scheme (65) with  $v(x)$  given by eq. (71) at  $D_{\text{eff}} = 1$ ,  $b = 3/2$ . The “noisy” line represents the result of stochastic simulation, the smooth line represents eq. (73).

Figure 12 depicts the comparison of the closed-form expression for the invariant density at  $b = 3/2$ ,  $D_{\text{eff}} = 1$  and the results of stochastic simulation of eq. (65).

### 4.3 Ergodicity breaking in higher dimensions

Ergodicity breaking occurs also in higher dimensional GPK models in the presence of attractive and periodic potentials. Consider a two-dimensional GPK process

$$d\mathbf{x}(t) = \mathbf{v}(\mathbf{x}(t)) dt + \mathbf{b}_{\chi_N(t)} dt \quad (74)$$

with  $\mathbf{b}_\alpha = b(\cos \phi_\alpha, \sin \phi_\alpha)$ ,  $\phi_\alpha = 2\pi(\alpha - 1)/N$ ,  $\alpha = 1, \dots, N$ ,  $A_{\alpha, \beta} = 1/N$ , and  $\lambda_\alpha = \lambda$ ,  $\alpha, \beta = 1, \dots, N$ , in the presence of a deterministic bias

$\mathbf{v}(\mathbf{x})$  stemming from a potential,  $\mathbf{v}(\mathbf{x}) = -\nabla U(\mathbf{x})/\eta$ , which corresponds to a typical transport problem under overdamped conditions, where  $\eta$  is the friction factor.

To begin with consider a harmonic, globally attractive, contribution

$$\mathbf{v}(\mathbf{x}) = -v_0 \begin{pmatrix} x \\ y \end{pmatrix} \quad (75)$$

deriving from the quadratic potential  $U(\mathbf{x}) = U_0(x^2 + y^2)/2$ , with  $v_0 = U_0/\eta$ , and set  $D_{\text{nom}} = b^2/2\lambda = 1$ , and  $v_0 = 1$ . Figure 13 depicts some orbits of GPK particles for several values of  $N$  and  $b$ . As can be observed particle motion is localized within an invariant region  $\Omega$  of the plane, the structure of which depends on the choice of the stochastic velocity vectors, i.e., on  $N$  and  $b$ .

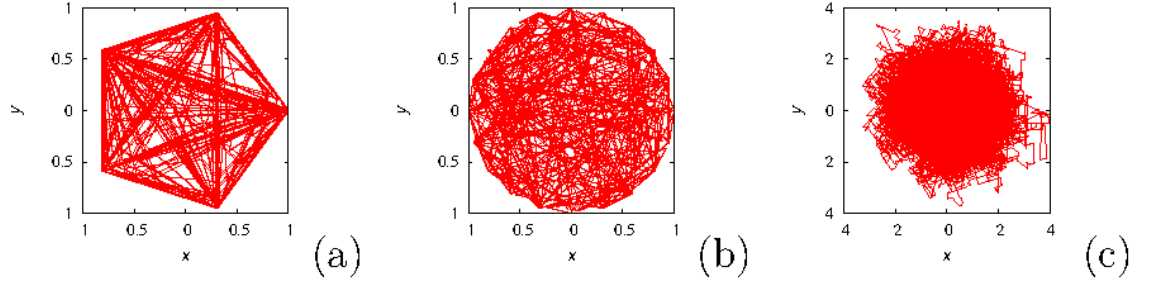


Figure 13: Orbits of the GPK process described in the main text in the presence of a two-dimensional attractive harmonic potential. Panel (a):  $N = 5$ ,  $b = 1$ ; panel (b):  $N = 20$ ,  $b = 1$ ; panel (c):  $N = 5$ ,  $b = 10$ .

The structure of the invariant domain  $\Omega$  can be derived from the condition of invariance, which dictates

$$(\mathbf{v}(\mathbf{x}) + \mathbf{b}_\alpha) \cdot \mathbf{n}_e(\mathbf{x})|_{\mathbf{x} \in \partial\Omega} \leq 0 \quad \forall \alpha = 1, \dots, N \quad (76)$$

at the boundary  $\partial\Omega$  of  $\Omega$ , where  $\mathbf{n}_e(\mathbf{x})$  is the outwardly oriented normal unit vector at  $\mathbf{x} \in \partial\Omega$ , and “ $\cdot$ ” indicates the Euclidean scalar product. By considering the radial symmetry of the potential, an invariant region (not the minimal one) can be sought as a circle of radius  $R$  around the origin. Let  $(r, \theta)$  be the radial coordinates. Since  $\mathbf{v}(\mathbf{x}) = -v_0 r \mathbf{e}_r$ , where  $\mathbf{e}_r$  is the unit radial vector, eq. (76) can be expressed as

$$-v_0 R + b \cos(\phi_\alpha - \theta) \leq 0 \quad (77)$$

$\alpha = 1, \dots, N$ ,  $\theta \in [0, 2\pi)$ , i.e.,

$$R \geq \frac{b}{v_0} \cos(\phi_\alpha - \theta) \quad (78)$$

that is certainly satisfied provides that  $R > R_c = b/v_0$ . The contour plots of the stationary invariant densities  $p_*(\mathbf{x})$  associated with two typical GPK processes depicted in figure 13 are shown in figure 14.

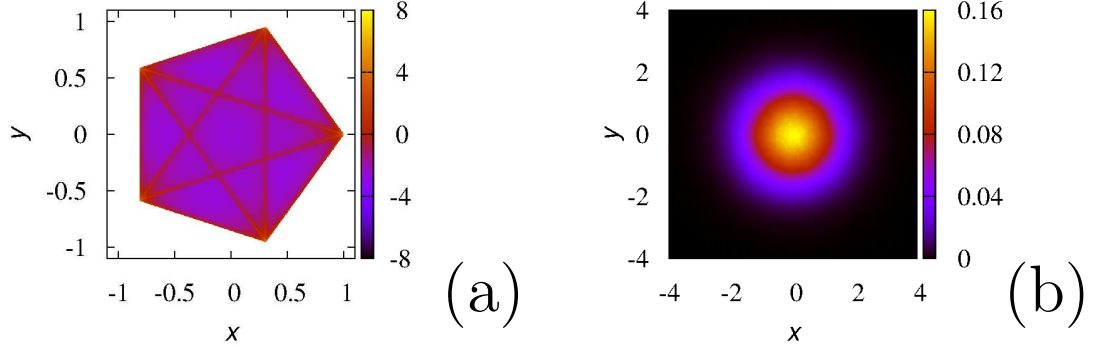


Figure 14: Contour plot of the compactly supported stationary invariant densities  $p_*(\mathbf{x})$  for GPK processes in the presence of a harmonic potential. Panel (a) refers to the contour plot of  $\log(p_*(\mathbf{x}))$  at  $N = 5$ ,  $b = 1$ , so that  $R_c = 1$ , panel (b) to the contour plot of  $p_*(x, y)$  at  $N = 5$ ,  $b = 10$ , thus  $R_c = 10$ .

For low values of  $b$  (panel a), the support of the invariant density strongly depends on the geometry of the stochastic velocity vectors (in this case, possessing a pentagonal shape, since  $N = 5$ ). For high values of  $b$ , the stationary invariant density does not depend on  $\{\mathbf{b}_\alpha\}_{\alpha=1}^N$ , and can be accurately approximated by the corresponding Kac-limit solution, that in the present case provides the expression

$$p_*(\mathbf{x}) = A \exp \left[ -\frac{U(\mathbf{x})}{\eta D_0} \right] = A \exp \left[ -\frac{v_0 (x^2 + y^2)}{2 D_0} \right] \quad (79)$$

where  $A$  is a normalization constant. Figure 15 depicts the stationary radial distribution function  $p_r^*(r)$ ,  $\int_0^\infty p_r^*(r) dr = 1$  in the cases considered above. For small values of  $b$  (panel (a),  $b = 1$ ),  $p_r^*(r)$  is essentially localized at the outer boundary, i.e., at  $r = R_c = 1$ , while for high  $b$ 's it practically coincides with the Kac-limit expression

$$p_r^*(r) = \frac{v_0}{D_0} r e^{-v_0 r^2 / 2 D_0} \quad (80)$$

This preliminary analysis of GPK processes in radially attractive potential is propaedeutical to the interpretation of ergodicity-breaking phenomena

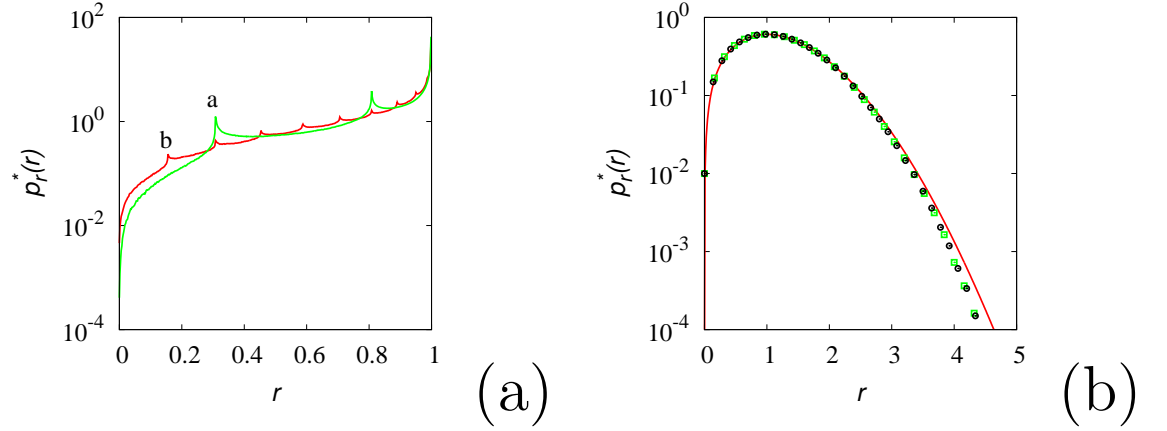


Figure 15: Stationary radial distribution  $p_r^*(r)$  vs  $r$  for GPK processes in the presence of a harmonic potential. Panel (a) refers to  $b = 1$ . line (a) corresponds to  $N = 5$ , line (b) to  $N = 10$ . Panel (b) to  $b = 10$ . Symbols ( $\circ$ ) correspond to  $N = 5$ , ( $\square$ ) to  $N = 20$ . The solid line is the Kac-limit expression for  $p_r^*(r)$  eq. (80).

in periodic potentials. Consider the GPK process (74) in  $\mathbb{R}^2$ , in the presence of a generic periodic potential  $\mathbf{v}(\mathbf{x}) = -\nabla U(\mathbf{x})/\eta$ , say

$$U(\mathbf{x}) = -\frac{U_0}{2\pi} \cos(2\pi x) \sin(2\pi y) \quad (81)$$

Set  $\eta = 1$ , and  $U_0 = 5$  for convenience, as the analysis of ergodicity breaking is qualitatively independent of the values attained by  $\eta$  and  $U_0$ , and set  $N = 20$ ,  $D_{\text{nom}} = 1$ . Figure 16 panel (a) shows the structure of the periodic potential (81) considered. Once  $D_{\text{nom}}$  is fixed, the only parameter of the model is the intensity  $b$  of the stochastic velocity fluctuations. For small values of  $b$ , below a given threshold  $b_{\text{crit}}$ , multiplicity of stationary invariant measures occur, corresponding to the presence of a countable system of invariant regions for the GPK process located around the local potential minima. This phenomenon is depicted in panel (b) of figure 16 representing some trajectories of GPK particles at  $b = 3$ , starting from several different initial positions that become trapped within the invariant regions around the local potential minima. The critical value  $b_{\text{crit}}$  depends linearly on the intensity of potential  $U_0$ . For  $b < b_{\text{crit}}$ , ergodicity breaking occurs. Above  $b_{\text{crit}}$ , that in the present case is approximately  $b_{\text{crit}} \simeq 3.59$ , GPK dynamics does not display multiplicity of localized stationary invariant measures, and ergodicity is recovered. The qualitative behavior of the orbits above the threshold  $b_{\text{crit}}$  is depicted in panels (c) and (d). For  $b \simeq b_{\text{crit}}$ , but above the threshold, as in panel (c) corresponding to  $b = 3.7$ , the orbits of GPK

particles are characterized by a “punctured dynamics”, characterized by longer residence times in the neighborhood of potential minima followed by sudden jumps towards one of the nearest neighboring minima. Conversely, for  $b \gg b_{\text{crit}}$ , as depicted in panel (d) for  $b = 10$ , GPK-particle orbits resemble those of a Brownian particle, and the influence of the potential involves the long-term dispersion properties, the quantitative analysis of which can be recovered from the Kac limit of the model, for sufficiently high values of  $b$ .

## 5 Concluding remarks

In this second part we have focused attention on the quantitative description of dissipation in GPK dynamics, both in terms of energy-dissipation functions (substantially corresponding to  $L^2$ -norms of the partial probability densities) and entropies.

A correct representation of these dissipation functions should necessarily take into account the primitive statistical formulation of the process, based on the full system of partial probability density functions  $\{p_\alpha(\mathbf{x}, t)\}_{\alpha=1}^N$ . No consistent energy dissipation or entropy functions can be formulated exclusively upon the knowledge of the overall probability density function  $p(\mathbf{x}, t)$ . This represents a qualitative stochastic confirmation of the basic ansatz underlying extended thermodynamic theories of irreversible processes. On the other hand, the analysis of higher dimensional GPK processes, ( $n > 1$ ), indicates that it is not possible to develop a consistent thermodynamic theory of dynamic processes possessing finite propagation velocity, by expressing thermodynamic state variables exclusively in terms of concentrations and their “diffusive” fluxes, as the whole systems of partial probability densities (concentrations) should be taken into account. This issue is further developed in part III.

We have also outlined another relevant application of Poisson-Kac and GPK processes as mollifiers of space-time stochastic perturbations in the analysis of field equations (stochastic partial differential equations). This application has been only sketched in Section 4, and hopefully Poisson-Kac mollification can lead to interesting physical and mathematical results, in the spirit of Wong-Zakai theorems and regularity-structures’ theory

Moreover, we have shown that ergodicity breaking, and the occurrence of multiple stationary invariant measures are generic properties of GPK dynamics in higher dimensional periodic potential, provided that the characteristic intensity  $b^{(c)}$  of the stochastic velocity vectors is below a critical threshold  $b_{\text{crit}}$  which depends on the intensity and on the structure of the potential barriers.



## References

- [1] Giona M, Brasiello A and Crescitelli S 2016 Stochastic foundations of undulatory transport phenomena: Generalized Poisson-Kac processes - Part I Basic theory, submitted to *J. Phys. A*
- [2] Kac M 1974 *Rocky Mount. J. Math.* **4** 497
- [3] Jou D, Casas-Vazquez J and Lebon G 1996 *Extended irreversible thermodynamics* (Berlin: Springer Verlag)
- [4] Müller I and Ruggeri T 2013 *Rational extended thermodynamics* (Berlin: Springer Verlag)
- [5] Jou D, Casas-Vazquez J and Lebon G 1999 *Rep. Prog. Phys.* **62** 1035
- [6] Giona M, Brasiello A and Crescitelli S 2016 Stochastic foundations of undulatory transport phenomena: Generalized Poisson-Kac processes - Part III Extensions and applications to kinetic theory and transport, submitted to *J. Phys. A*
- [7] Chirikov B V 1979 *Phys. Rep.* **52** 263
- [8] McKay R S, Meiss J D and Percival I C 1984 *Physica D* **13** 55
- [9] Guerra F 1981 *Phys. Rep.* **77** 263
- [10] Adler R J and Taylor J E 2007 *Random fields and geometry* (Berlin: Springer Verlag)
- [11] Giona M, Brasiello A and Crescitelli S 2015 *Europhys. Lett.* **112** 30001
- [12] Camacho J and Jou D 1992 *Phys. Lett. A* **171** 26
- [13] Vlad M O and Ross J 1994 *Phys. Lett A* **184** 403
- [14] Cimmelli V A, Jou D, Ruggeri T and Van P 2014 *Entropy* **16** 1756
- [15] Seneta E 2006 *Non-negative matrices and Markov Chains* (New York: Springer Science & Business Media)
- [16] Giona M 2016 Covariance and spinorial statistical description of simple relativistic stochastic kinematics, in preparation
- [17] Giona M 2016 Relativistic analysis of stochastic kinematics, in preparation
- [18] Giona M, Adrover A, Cerbelli S and Vitacolonna V, 2004 *Phys. Rev. Lett.* **92** 114101

- [19] de Groot S R and Mazur P 1984 *Non-equilibrium thermodynamics* (New York: Dover Publ.)
- [20] Wong E and Zakai M 1965 *Int. J. Eng. Sci.* **3** 213
- [21] Wong E and Zakai M 1965 *Ann. Math. Stat.* **36** 1560
- [22] Konecny F 1983 *J. Multivariate Anal.* **13** 605
- [23] Twardowska K 1996 *Acta Appl. Math.* **43** 317
- [24] Hairer M and Pardoux E 2015 *J. Math. Soc. Japan* **67** 1551
- [25] Milonni P W 1994 *The quantum vacuum: an introduction to quantum electrodynamics* (Boston: Academic Press)
- [26] Lyons T J 1998 *Rev. Mat. Iberoamericana* **14** 215
- [27] Friz P K and Hairer M 2014 *A Course on Rough Paths* (New York: Springer Science & Business media)
- [28] Edwards S F and Wilkinson D R 1982 *Proc. R. Soc. London Ser. A* **381** 17
- [29] Antal T and Racz Z 1996 *Phys. Rev. E* **54** 2256

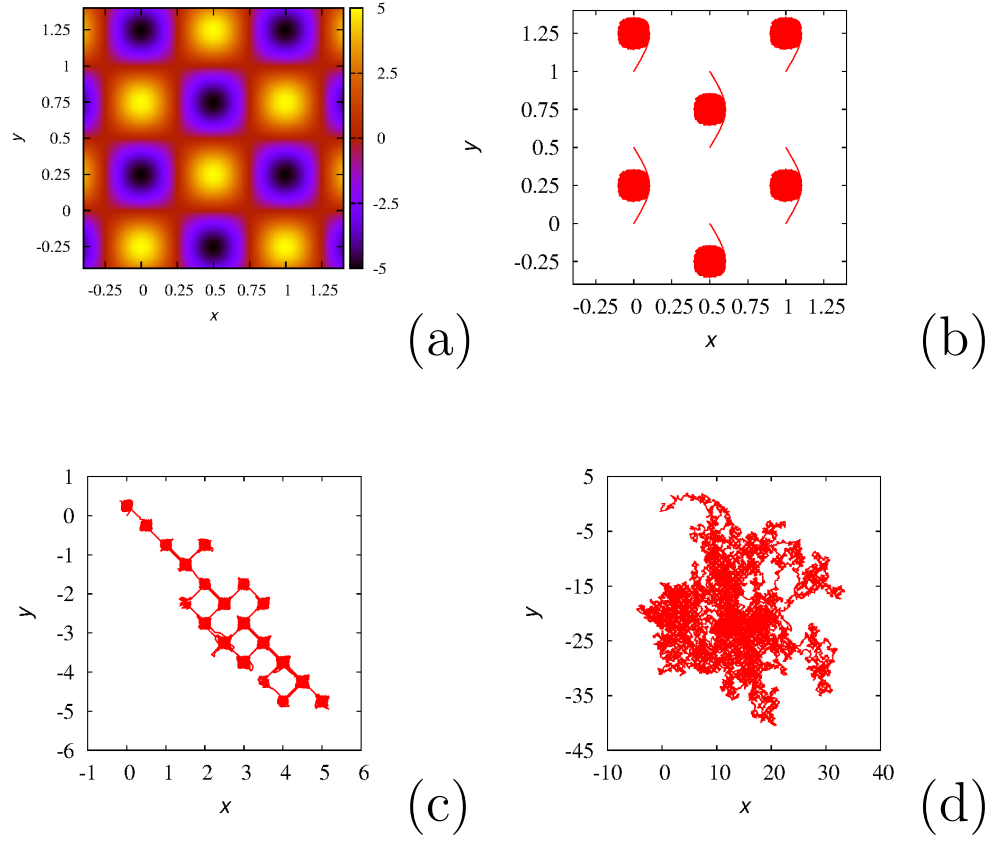


Figure 16: Panel (a): Contour plot of the periodic potential (81). Panel (b):  $b = 3$ , orbits of the GPK process starting from different initial positions. Panel (c):  $b = 3.7$ , generic orbit of the GPK process. Panel (d):  $b = 10$ , generic orbit of the process.